Fischer-Tropsch Synthesis

Lucas Brübach, Moritz Wolf, and Peter Pfeifer

Abstract For the production and utilization of powerfuels, particularly hydrocarbon-based power-to-liquid (PtL) fuels like kerosene and diesel, the Fischer-Tropsch (FT) synthesis is seen as an essential technology and pathway in recent and upcoming years. Starting from carbon dioxide (CO_2) as a primary source for producing the fuels in a carbon neutral pathway, FT has the advantage to eliminate the oxygen molecules directly in the fuels synthesis by producing water as byproduct. The latter could be recycled for generating hydrogen through electrolysis. Also, fuel composition matches quite well to the current standards and regulations such as ASTM 7566-1 and DIN EN 15940 exist for blending hydro-processed FT syncrude product to kerosene and diesel fuel into existing turbine and motor fleet, respectively. The chapter on FT is focussing on the recent developments of reactor technology for process intensification and integration regarding CO_2 activation with specific attention to volatility of the hydrogen source when hydrogen is produced from renewable electricity.

Keywords Fischer-Tropsch synthesis · Process intensification · Reactor technology · Process integration · CO_2 activation · Fluctuating feed/Dynamic operation

L. Brübach
Karlsruhe Institute of Technology (KIT), Institute for Micro Process Engineering (IMVT), Karlsruhe, Germany

M. Wolf
Karlsruhe Institute of Technology (KIT), Institute of Catalysis Research and Technology (IKFT) and Engler-Bunte-Institute (EBI), Karlsruhe, Germany

P. Pfeifer (✉)
INERATEC GmbH, Karlsruhe, Germany
e-mail: peter.pfeifer@ineratec.de

1 Introduction

For the production and utilization of powerfuels, particularly hydrocarbon-based power-to-liquid (PtL) fuels like kerosene and diesel, the Fischer-Tropsch (FT) synthesis is seen as an essential technology and pathway in recent and upcoming years. Starting from carbon dioxide (CO_2) as a primary source for producing the fuels in a carbon neutral pathway, FT has the advantage to eliminate the oxygen molecules directly in the fuels synthesis by producing water as byproduct. The latter could be recycled for generating hydrogen through electrolysis. Also, fuel composition matches quite well to the current standards and regulations such as ASTM 7566-1 and DIN EN 15940 exist for blending hydro-processed FT syncrude product to kerosene and diesel fuel into existing turbine and motor fleet, respectively.

Nevertheless, the application and development of this technology date back to the last century already. Since its discovery in the early nineteenth century, the Fischer-Tropsch synthesis (FTS) has always received huge interest whenever crude oil was scarce due to geographical, economical, or political reasons.[1] The Fischer-Tropsch process was first commercialized and intensively used by the Nazi regime in Germany in the 1930s with the goal of industrial autarky preceding World War II. Synthetic fuels were produced from coal in a coal-to-liquid (CTL) process including FTS, which was adapted by the South African government during apartheid due to sanctions. The oil crisis in the 1970s and the price hike of crude oil in recent decades again put FTS in the spotlight for alternative production of fuels from other fossil resources than oil, while in particular natural gas became the primary feedstock for commercial applications of FTS via a gas-to-liquid (GTL) approach. However, the strong link of the profitability in the production of FTS products to the crude oil price always rendered investments into new large-scale FTS plants risky.

Eventually, the urgent need in seeking sustainable alternatives to fossil energy sources due to climate change revived the FTS technology once again, at first focusing on biomass as a renewable feedstock (biomass-to-liquid, BTL) and later using CO_2 and green electricity via the power-to-liquid (PtL) route. In this context, i.e., for the deployment of FTS technologies for PtL fuel production in the upcoming years, an in-depth understanding and assessment of precise process conditions and specifications is crucial. This includes key areas such as

- process combinations to activate CO_2,
- understanding catalyst optimization,
- reactor technologies to improve process efficiency, and
- challenges of fluctuating renewable energy on reactor and process level.

However, in this field, comparative studies are somewhat limited. Thus, this chapter aims to provide a broader overview of the specifics in FTS processes by consolidating research results from respective individual studies.

2 Traditional Fischer-Tropsch process

The overall classical Fischer-Tropsch process consists of four major steps: production of synthesis gas, cleaning/purification of synthesis gas, the actual FT synthesis step, and product conditioning (Fig. 1). All carbonaceous sources, such as coal, natural gas, biomass, or organic wastes may be reformed or gasified yielding synthesis gas. However, the particular processes and process conditions strongly vary for different raw materials. For instance, due to high ash contents in biomass and coal, the purification of synthesis gas from biomass or coal gasification is much more elaborate than for synthesis gas from steam reforming of natural gas [1, 2]. In regard to the FTS, a high temperature (320–350 °C) and a low temperature (220–250 °C) pathway are commercially established [3], while a medium temperature Fischer-Tropsch (MTFT) process (270–290 °C) has recently been commercialized by Synfuels China [4, 5].

2.1 Heterogeneous Catalysts

Franz Fischer and Hans Tropsch reported that group VIII metals were capable of activating carbon monoxide (CO) hydrogenation, while only iron, cobalt, and nickel were identified as viable catalytic material [7]. Iron showed a superior performance at 350–500 °C, while a decreased temperature range of 250–270 °C was observed for cobalt. For nickel, only a reduction of the reaction temperature to 160 °C resulted in a reasonable methane selectivity [7]. Combinations of these active metals with an equal or three times higher amount of aluminum, beryllium, chromium, magnesium, manganese, uranium, or zinc in their oxidic phase, but also the addition of silicic acid, rare earth (RE) metal oxides, activated carbon, or amorphous carbon was tested for a promotional effect accordingly. Especially the metal oxides had a beneficial effect on the catalytic behavior, while the addition of palladium, copper, and iron oxide to nickel and cobalt enhanced their performance [7].

These early findings are still in line with nickel being the metal of choice for industrial methanation and an exclusive commercial application of iron-based catalysts

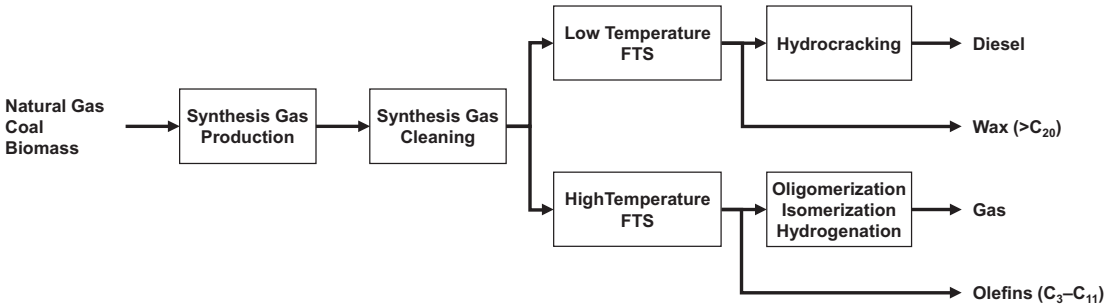

Fig. 1 Scheme of the overall process for the production of synthetic liquid fuels and other hydrocarbons by the Fischer-Tropsch synthesis. Reproduced from Guettel et al. [6]

in the high-temperature Fischer-Tropsch synthesis (HTFTS) [8, 9]. The catalysts are typically chemically promoted by K_2O and contain structural promoters such as magnesium oxide (MgO) or aluminum oxide (Al_2O_3). However, iron catalysts have been significantly improved and are nowadays, together with cobalt-based catalysts, also applied in the low-temperature Fischer-Tropsch synthesis (LTFTS) [8, 9]. In case of Sasol for instance, a major global company in FTS technology, a typical iron-based catalyst for LTFTS contains Fe, SiO_2, Cu, and K_2O with a 20:5:1:1 mass ratio [10]. One major characteristic of iron-based catalysts is their water–gas shift activity allowing for the use of hydrogen (H_2)-poor synthesis gas feeds as obtained from the gasification of coal. The conversion of CO to the favor of H_2 via the water–gas shift reaction is typically thermodynamically controlled under FT conditions [11, 12, 13]. In contrast, this reaction path is mostly negligible for cobalt-based FT catalysts, but a pronounced formation of methane is observed over cobalt-based catalysts, especially at increased temperatures [11, 12, 13]. The first commercial cobalt-based catalysts in the German coal-to-liquid (CTL) plants were promoted by thorium, zirconium, or magnesium and mixed with Kieselguhr, a siliceous sedimentary rock, at a 1:1 mass ratio [14]. Nowadays, cobalt is typically supported on (mostly modified) large surface area metal oxide supports such as aluminum oxide (Al_2O_3), silicon dioxide (SiO_2), and titanium dioxide (TiO_2), while platinum (Pt), rhenium (Re), or ruthenium (Ru) are applied as reduction promoters. Lanthana, zirconia, or alkali oxides represent common structural oxidic promoters [15, 16, 17].

Cobalt-based catalysts are more expensive and active than iron-based catalyst [18]. An increased mass-specific activity over the lifetime of approximately two magnitudes is required and achieved via utilization of supported nanoparticles, i.e., by increasing the specific surface area of the active cobalt phase drastically. In contrast, fused or precipitated, rather bulky iron-based catalysts are typically applied as a commercial catalyst due to the low price of iron-based ores [8, 18].

2.2 Reactions and Product Distribution

The broad product spectrum is one of the major characteristics of the FTS and includes hydrocarbon chain lengths of more than 100. Paraffins, olefins, oxygenates, and aromatics are all primary organic products. The reaction proceeds via in situ produced monomers in a polymerization-type mechanism. Hence, the reaction pathway includes the generation of a chain initiator, which is followed by chain growth or propagation. Subsequent chain growth termination or simple desorption results in the (intermediate) products. A representative overall reaction may be described as the hydrogenation of CO forming a (CH_2) hydrocarbon chain segment and water (H_2O) (Eq. 1) [10, 12]. A general reaction equation for the formation of paraffins (Eq. 2) and olefins (Eq. 3) can be formed as well.

$$CO + 2H_2 \rightarrow (CH_2) + H_2O \tag{1}$$

$$n\mathrm{CO} + (2n+1)\mathrm{H_{2^-}} \rightarrow \mathrm{C}_n\mathrm{H}_{(2n+2)} + n\mathrm{H_2O} \tag{2}$$

$$n\mathrm{CO} + 2n\mathrm{H_2} \rightarrow \mathrm{C}_n\mathrm{H}_{2n} + n\mathrm{H_2O} \tag{3}$$

The required stoichiometric composition of the reactants H_2 and CO in the synthesis gas feed decreases with the average chain length in the final product mixture [19, 20]. Methanation (Eq. 4) and the water–gas shift (WGS) reaction (Eq. 5) are the most important side reactions in the FTS [19, 20]. Thermodynamically, methane is the most stable hydrocarbon under FT conditions. However, the FT reaction is kinetically controlled allowing for the formation of other hydrocarbons as well. Therefore, the main reactions of the FTS are far away from the thermodynamic equilibrium [12, 21].

$$\mathrm{CO} + 3\mathrm{H_2} \leftrightarrow \mathrm{CH_4} + \mathrm{H_2O} \tag{4}$$

$$\mathrm{CO} + \mathrm{H_2O} \leftrightarrow \mathrm{CO_2} + \mathrm{H_2} \tag{5}$$

The exact FT mechanisms are one of the most discussed topics in heterogeneous catalysis with various proposed pathways. It is generally understood that a number of parallel pathways exist; i.e., a combination of proposed mechanisms may describe the FTS best [9, 19, 20, 22–26]. The four most popular mechanisms are the alkyl mechanism, the alkenyl mechanism, the enol mechanism, and the CO-insertion mechanism [22]. They all propose a step-wise chain growth as the product distribution can be predicted by a chain growth probability [10, 14].

The chain growth probability depends on the reaction conditions such as the overall pressure, the temperature, or the composition of the gas phase, and strongly on the catalysts. For the industrial LTFTS, a probability exceeding 90% is desired to mostly produce long-chained hydrocarbons, while the probability in the HTFTS is typically in the range of 70–75%.[10] Idealized, statistical models to calculate the product distribution for reactions like polymerizations have been developed. The Anderson-Schulz-Flory model (ASF) has been widely accepted as descriptor of the FT product spectrum (Fig. 2).

In the ASF model, a chain growth probability (p_G) is determined by the rates of chain growth (r_{cg}) and chain growth termination (r_{cgt}; Eq. 6). Aside from the actual chain length (N_C), this probability is the only parameter in the calculation of the selectivity of the particular chain lengths ($S_{N,C}$; Eq. 7) [22, 27].

$$p_G = \frac{r_{\mathrm{cg}}}{r_{\mathrm{cg}} + r_{\mathrm{cgt}}} \tag{6}$$

$$S_{N,C} = (1 - p_G)p_G^{N_C - 1} \tag{7}$$

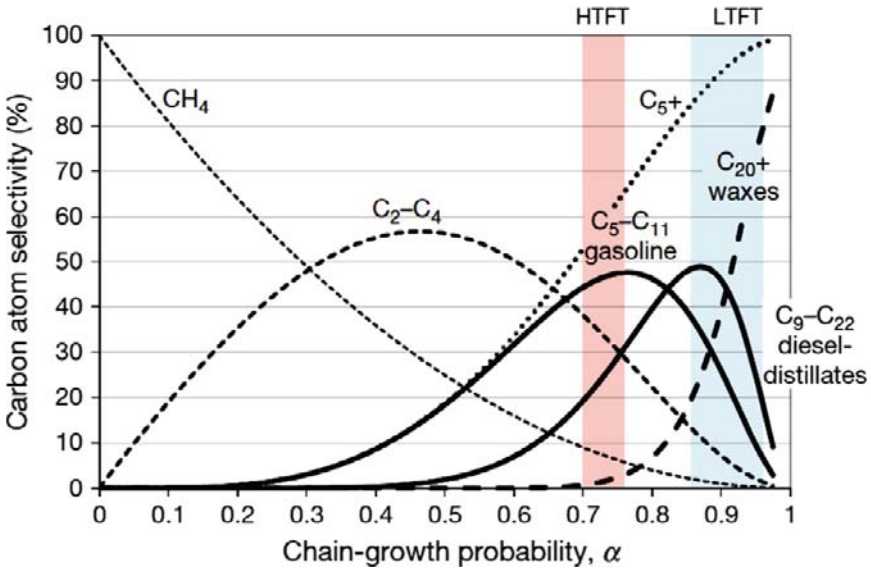

Fig. 2 Hydrocarbon product spectrum according to the Anderson-Schulz-Flory (ASF) model with regimes for the chain growth probability for the commercial HTFT and LTFT. Reproduced from van de Loosdrecht et al. [16]

2.3 Traditional Reactor Solutions

Commercial FT reactors are typically operated with heterogeneous catalysts. The most important reactor designs (Fig. 3) for the high-temperature Fischer-Tropsch synthesis (HTFTS) are the circulating and the fixed fluidized bed reactors. Multi-tubular fixed bed reactors and slurry phase bubbling reactors are preferred for the low-temperature Fischer-Tropsch synthesis (LTFTS) [3]. The released energy of the highly exothermic FT reaction is equal to around 25% of the heat of combustion of the input synthesis gas [12]. Removing this heat of reaction from the FT reactor is of utmost importance in order to avoid thermal degradation of the catalyst by overheating, as well as associated undesired selectivity changes, such as an increased methane yield. The selectivity is strongly temperature-dependent, and hence, an ideal isothermal reactor is mandatory to control the product distribution [3].

3 Fischer-Tropsch Processes for Powerfuels

The overall process layout for producing powerfuels from carbon dioxide can heavily determine the approach in which Fischer-Tropsch is conducted. Currently, the following process step combinations, as shown in Table 1 and Fig. 4, are being discussed.

For most process combinations, examples can be found in recent research. Moreover, the Fischer-Tropsch process seems advantageous with cobalt as active catalyst

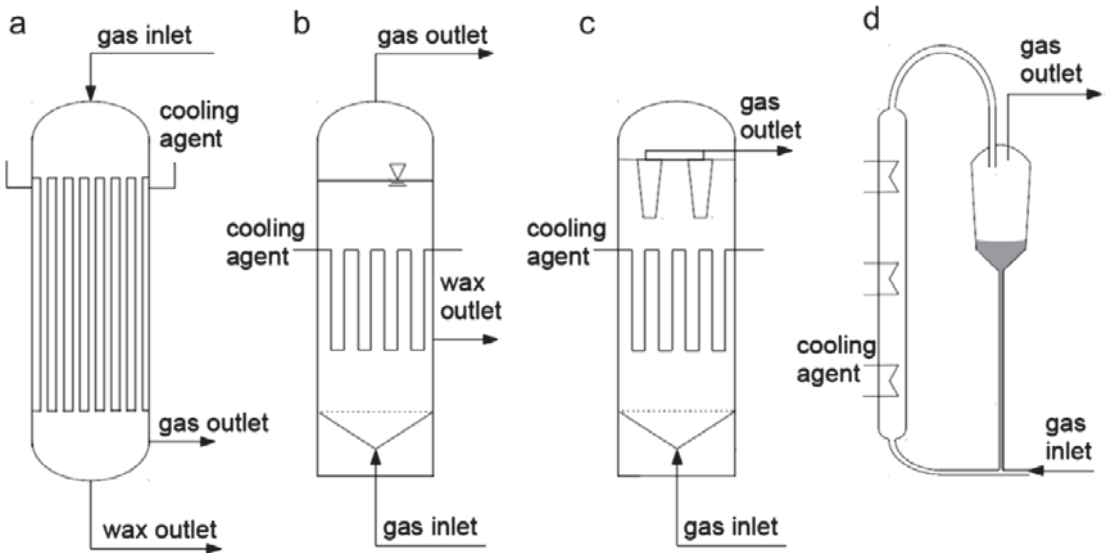

Fig. 3 Schematics of major large-scale Fischer-Tropsch reactors: **a** multi-tubular fixed bed reactor, **b** slurry phase bubbling reactor, **c** fixed fluidized bed reactor, and **d** circulating fluidized bed reactor

Table 1 Overview of main Fischer-Tropsch (FT) process step combinations

FT process variant		Description
1	Water electrolysis, rWGS, and FT	Water electrolysis in proton exchange membrane (PEM) or alkaline (AE) cells, summarized as water electrolysis, for hydrogen production combined with reverse water–gas shift (rWGS) and FT
2	Direct activation of CO_2	Water electrolysis in PEM or AE and simultaneous activation of CO_2 and FT synthesis in a single reactor (often called CO_2-FT or direct activation of CO_2)
3	SOEC steam electrolysis, rWGS, and FT	Steam electrolysis in solid oxide electrolyzer cells (SOEC) for hydrogen production combined with rWGS and FT, whereas steam is exported from FT to feed the electrolysis
4	SOEC co-electrolysis of CO_2 and steam and FT	Co-electrolysis of CO_2 and steam in SOEC for synthesis gas production combined with cobalt-based FT, whereas steam is exported from FT to feed the electrolysis
5	Separate CO_2 and H_2O electrolysis plus FT	Electrolysis of CO_2 in PEM or SOEC to generate CO for co-feeding to hydrogen from other electrolysis for FT
6	CO_2 plasma splitting and electrolysis plus FT	Plasma splitting of CO_2 to generate CO for co-feeding to hydrogen from other electrolysis for FT
7	CO_2 plasma splitting, WGS, and plus FT	Plasma splitting of CO_2 to generate CO and the water–gas shift (WGS) to form additional hydrogen from parts of the CO for FT

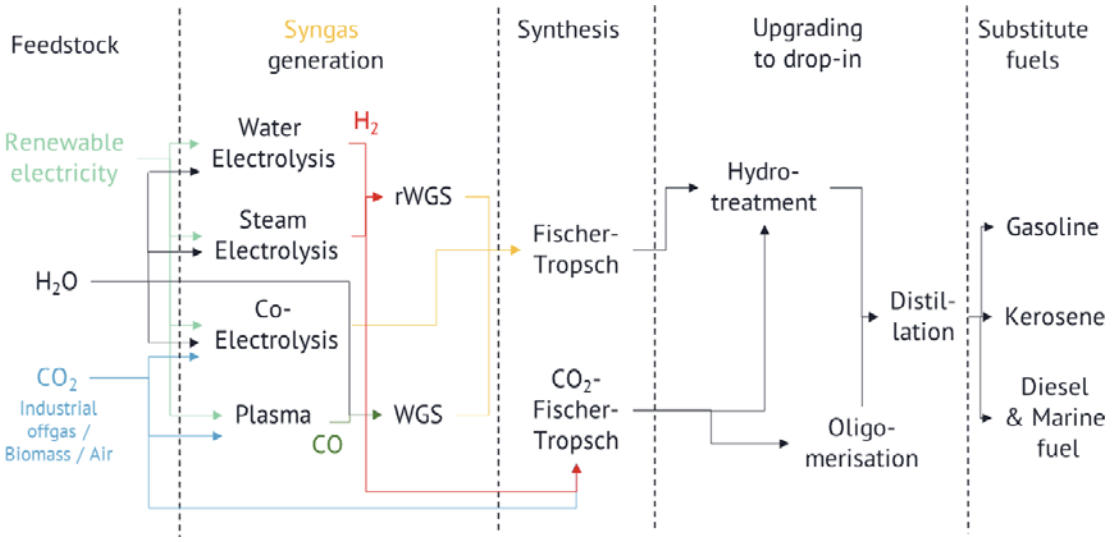

Fig. 4 Process variants for conduction of FT from renewable power and CO_2 with simplified view on the syncrude upgrading to fuels

for all these combinations because different but commonly above or near the thermodynamic CO concentration at temperature up to 300 °C may be present from the preceding processes in the feed gas of the FT. As such, water–gas shift, a possible side reaction on iron catalyst, would often reduce the CO level than increasing it. A recycle over the FT reactor may be required if no process intensification is performed. In such case, low conversions of CO are required to prevent hot-spots or an overall high steam partial pressure in the reactor. Both would lead to accelerated catalyst deactivation. Such necessary recycle would be additional to any required recycling of unreacted CO_2 in the preceding processes of CO generation for high carbon utilization. To avoid the FT recycle, process intensification can be applied.

The following sections will elaborate on the current trends in process intensification for Fischer-Tropsch processes, as presented in Table 1, with focus on cobalt catalysts and reactors. Nevertheless, the following list will introduce the overall processes and provide some general aspects.

- Process variant #1 is the most common one. As water electrolysis is state-of-the-art, different companies like INERATEC GmbH or Haldor Topsoe A/S apply reverse water–gas shift to obtain syngas with H_2/CO of 2:1 from a H_2/CO_2 molar mixture 3:1. This process variant is also quite frequently investigated in research. It has been explored, e.g., in the BMWi-funded PowerFuel project [28] under the aspects of transient operation along the process chain containing DAC, PEM electrolysis, rWGS, and FT together with upgrading of the synthetic crude product to kerosene. The aspect of transient operation in the FT synthesis will be discussed in the subsection "The Aspect of Transient Operation in PtL" (Sect. 4). The project partners Siemens Energy, Karlsruhe Institute of Technology (KIT), INERATEC GmbH and Climeworks AG utilized KIT's Energy Lab 2.0 infrastructure [29] to investigate the process chain, which also currently serves for the Kopernikus Power-to-X project.

- A specialty from the topic of process intensification may be process variant #2; there, process integration is the key factor. The direct route has recently gained attention through the intended avoidance of the high-temperature rWGS process for CO_2 activation and will be discussed in the section "Process Integration of rWGS and FT" (Sect. 3.4). Nevertheless, the upgrading could be more complex than in standard cobalt-based FTS due to the obtained rather short hydrocarbon chain length.
- Process variant #3 is frequently discussed to improve the overall process efficiency through the higher Faradaic efficiency of steam electrolysis in solid oxide electrolyzer cells (SOEC) versus water electrolysis. Heat from the exothermic FT process can further be utilized to generate the steam. Thus, beneficial combination of individual steps in the overall process is possible. At Energy Lab 2.0 [29] at Karlsruhe Institute of Technology (KIT) such combination is established and could be investigated further.
- A further example for research on the above process combinations is the BMBF-funded Kopernikus Power-to-X project [30] assembling the worlds' first complete process of CO_2 direct air capture (DAC) with Co-SOEC and FT system. Within the project, the partners KIT, INERATEC GmbH, Climeworks, and Sunfire GmbH showed that there is evidence of much higher overall efficiencies through coupling these process steps. Around 50 L of liquid already hydro-processed FT crude has been produced with this process combination. Heat, effectively recovered in microstructured FT reactors, could be delivered for steam generation of the SOEC system and residual heat to CO_2 desorption, a special benefit of process variant #4.
- Process variant #5 separates H_2 and CO supply to the FT process. For generation of both molecules, different types of electrolysis may be applied, i.e., low- or high-temperature type. It has been suggested that CO could be produced in similar arrangements like water electrolysis or SOEC cells in different projects. Separating the two feed streams could be beneficial in terms of complexity over co-electrolysis as CO could be sequestrated from unconverted CO_2 after the electrolysis. Nevertheless, this would not allow recycling of gaseous species from FT into a preceding process and thus reduce carbon efficiency for C_{5+} species. To our knowledge, no example for this process variant is known.
- Plasma splitting is also frequently under debate to serve CO for downstream processes like FT. Process variant #6 is also a separate supply approach for CO and H_2 while using plasma splitting of CO_2 for CO production. However, from literature only process variant #7 is known. In the EU project Kerogreen, the world's first assembly has been evaluated following this process variant. Figure 5 shows the assembly together with the project partners' contributions. CO and O_2 are produced through plasma splitting, while oxygen is separated in an electrochemical membrane system [31]. Unreacted CO_2 is recovered in a pressure swing adsorption. To generate synthesis gas, two-thirds of the CO is converted by a sorption-enhanced WGS (SE-WGS) with steam into CO_2 and H_2 for obtaining a H_2/CO ratio of 2 while simultaneously adsorbing and recovering CO_2 [32]. Further FT is used to produce syncrude, which is hydrocracked in situ to a kerosene

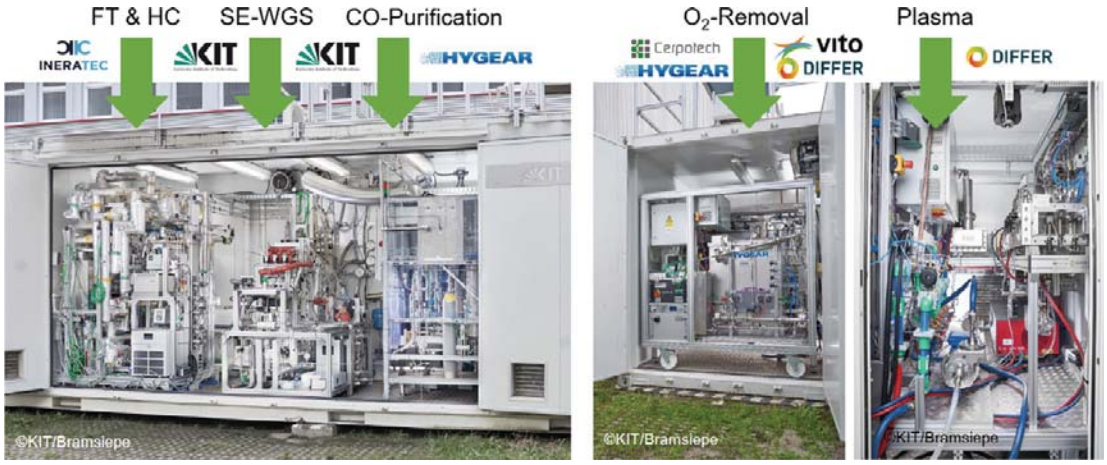

Fig. 5 Process variant 7 as demonstrated by Kerogreen's project partners [34]

pre-product [33]. Since the electrochemical cell for oxygen removal was not in the desired size, the overall process could not be fully evaluated. However, an upstream and downstream process testing was performed successfully.

In the following subsections, different aspects and approaches for process intensification and integration will be elaborated under the aspect of PtL technology. After a short section about catalyst insights and improvements, several sections will be devoted to different reactor designs and approaches with the FT core process.

3.1 Catalyst Improvement Through Operando Spectroscopy

Catalyst improvement is also a key factor for commercial viability of methods for process intensification as higher catalyst activity and selectivity are reducing capital expenditures for advanced reactor design through minimizing reactor size. Reduced holdup using more active and selective catalysts enables also reduced costs for operation and feedstock. This chapter does intend to detail recent advances around FT catalysts, since there are already elaborated studies on several aspects available, e.g., by Wolf et al. [35] or Suo et al. [36, 37]. Nevertheless, operando spectroscopy is shortly introduced as it can help to further understand and intensify FT for PtL application.

Ravenhorst et al. [38] used operando spectroscopic techniques for Co/TiO_2 catalysts, which account for nearly half of the world's transportation fuels produced by Fischer-Tropsch catalysis. Being able to obtain a spatial resolution of approximately 50 nm, they showed the interdependence of formed hydrocarbon species on the catalyst valence state. Their observed trends showed furthermore intra- and interparticular heterogeneities previously believed not to occur in particles below 200 μm. Capturing the genesis of an active FTS particle over its propagation to steady-state operation, they conclude that hydrocarbon deposits (differing in their

chemical composition) form a film on the surface of the catalyst particle, with inter- and intraparticle heterogeneities. These heterogeneities can be correlated to slight changes in the local Co oxidation/valence states also influenced by the H_2/CO ratio.

These observations are in line with operando deactivation studies by Loewert et al. [39] at a synchrotron radiation facility. They investigated a commercial Co/alumina catalyst over 300 h under harsh FT conditions (250 °C, 30 bar) including a detailed analysis of the resulting liquid products. They found that within the first hours on stream, the initial state of reduced Co remained without detecting any pronounced structural changes on the catalyst. With knowledge of a high C_{5+} selectivity, they conclude that the formation of a liquid film on the catalyst particles leads to decreasing catalytic activity due to mass transport limitations. In the following 8–80 h of operation, near-edge XANES spectra evidenced the formation of $CoAl_2O_4$. Furthermore, the ongoing increase in methane selectivity accompanied by the decline in C_{5+} selectivity was attributed from the authors to the filling of the catalyst pores by liquid products, which was still ongoing, leading them to the conclusion that the deactivation originated from a combination of changes in mass transport and solid-state reactions in this activity regime. Finally, they identified in the last hours of operation a third regime, in which no change of the Co state nor selectivity change occurred. Finding ideal graphitic carbon depositions on the catalyst by Raman spectroscopy after the long-term experiments leads them to the conclusion that long-term deactivation originates from a carburization process.

Fischer and Claeys [40] wrapped up some recent studies on operando spectroscopy and also highlighted the importance of such techniques to study catalyst deactivation [35, 41, 42]. Their conclusion might ideally summarize what can be expected from such kinds of studies. Well-designed laboratory-based in situ characterization techniques, such as XRD, magnetometry, and XAS, with representative hydrodynamics provide fully relevant kinetic data. Further, these methods could play an important role in the development of understanding of the FT process.

Through the availability of operando technology, extensive research is enabled and could provide a solid ground for further improvement on catalysts. Being able to observe the deactivation mechanism, one can expect that material science can help to reduce the need for catalyst exchange. Long catalyst life is a further key for costs associated with catalyst exchange and constant product quality. Reducing the requirement for increasing the temperature to cope for catalyst deactivation typically reduces the C_{5+} selectivity and thus the total output of a PtL plant. Avoiding "intrinsic" carbon formation on the Co catalyst is only one aspect. The role of specific sites for improved C_{5+} selectivity leading to a higher wax yield and thus a greater kerosene output after hydrocracking is another aspect, which is investigated in current projects like BMBF-funded CARE-O-SENE [43]. Further, the importance of the water byproduct on the oxidation or sintering of the catalyst, which is nowadays largely suppressed by applying mono-modal Co crystallite size slightly above 8 nm in industrial catalysts [41, 44, 45], could potentially be solved differently. This also applies for oxidation via solid-state reaction with the metal oxide support forming mixed cobalt oxides, which may be hindered via (surface) modification of the support [35].

3.2 *Reactor Technologies*

3.2.1 Microstructured or Microchannel Reactors

Microstructured devices were already introduced in the 1990s as potential technology to enhance heat and mass transfer [46]. Following the principle of process intensification, introduced by the 1st International Conference on Process Intensification for the Chemical Industry [47, 48], the microstructured technology takes advantage of the short heat and mass transfer distance within the tiny structures and, moreover, the large surface to volume ratio. It has been explored largely for enhancing chemical processes from batch to continuous processes [36]. Microchannel reactors have been proposed as a tool for enabling greener processes [49], for being applied for commercial size [50], and are more recently reviewed under the aspect of process intensification in the catalytic conversion of natural gas to fuels and chemicals [51].

One of the first published comparisons of a microstructured reactor with a highly diluted fixed bed by Myrstad et al. [52] clearly shows the advantage of the microsystem. Packed with undiluted catalyst of near industrial recipe, the selectivity did not differ from the highly diluted fixed bed, meaning that the catalyst is operated in near isothermal regime and is not influenced by any wall effects, neither side reactions on the large surface area nor wall slip effects were measurable. They also showed that the pressure drop in such catalyst-packed systems is tolerable. Piermartini et al. [53] intensified this study and varied the microchannel size with catalyst packing. They conclude that microstructures have two major advantages over a slurry bubble column: no backmixing suppressing catalyst deactivation through water vapor and a high selectivity by being able to work at high single pass conversion leading to an intrinsic high chain growth probability at a H_2/CO ratio of 1.8. Even at larger slit sizes of 1.5 mm the superior heat transfer leads to a high chain growth probability.

Knochen et al. [54] provided some design aspects for the millistructure-like systems under the aspect of process intensification. Alongside with the experimental verification, they used a modeling of the system and concluded that a particle size range of 100–350 μm and channel width of 1.5–3.0 mm are interesting options for commercial FT applications. In their study, the reactor productivity is the largest with 1.5 mm slit size. The catalyst productivity is larger for a 3.0 mm slit size, mainly due to slight over-temperatures which are of course on expense of the selectivity. Chambrey et al. [55] came to similar conclusions when comparing a standard fixed bed with a milli-fixed bed. Moreover, they highlighted that an uncontrolled temperature increase during the reactor startup seems to be a common problem of FT synthesis in the standard fixed bed reactors. This temperature increase during the reactor startup can lead to catalyst deactivation. Interestingly, Chambrey et al. [55] also found a similar conclusion on suppressed long-term catalyst deactivation in the milli-type reactor as Piermartini et al. [53] but compared to a stirred tank reactor. Nevertheless, they explained the difference by the cobalt reduction procedure and not via the water vapor backmixing effect on the catalyst.

Catalyst incorporation by coating for FT synthesis is proposed in several studies. For example, the study of Chin et al. [56] proposed aligned carbon nanotube arrays for microchannel systems. In their study, they produced carbon nanotubes grown on FeCrAlY foam structures with Al_2O_3 coating. Since the catalyst preparation involved combined methods of metal-organic chemical vapor deposition (MOCVD), catalytic nanotube growth, and dip-coating of Co catalyst components, this technology seems rather complex. Although they were able to demonstrate an increase in Fischer-Tropsch synthesis activity by a factor of four when compared to an engineered catalyst structure without the carbon nanotube arrays, the catalyst stability might limit commercial viability. Again, this study showed that improved mass and heat transfer allow for operation of the Fischer-Tropsch synthesis at higher temperatures without selectivity runaway favoring methane formation.

Almeida et al. [57, 58] also studied the coating but with a simple standard wash-coating procedure for cobalt catalysts. They demonstrated that with different catalyst coating thickness, a good selectivity for C_{5+} can be achieved during FT synthesis due to the excellent temperature control of the microchannel technology. Nevertheless, they also found that the coating thickness can influence the selectivity for both C_{5+} and olefin/paraffin ratio. Thus, it can be concluded from their study that industrial relevant thicknesses to reach a high reactor productivity [59] discourages the use of coatings because they tend to get inefficient. Ying et al. [60, 61] also conducted a study on washcoating of a microchannel structure with cobalt catalyst. They obtained a 0.8 g g^{-1} h^{-1} C_{5+} catalyst productivity. However, this is also not converted to reactor productivity, which would be required to detail this regarding commercial viability. Sun et al. [62] performed research on coated iron catalyst for determining the kinetics. Even though they were able to show a methane selectivity as low as 6.5%, the application of coatings seems quite far from application.

Generally, a broad range of geometric configurations within the microstructure are proposed to enable higher conversion per pass and higher selectivity to C_{5+} applying packed microsystems. For example, a fractal geometry was suggested by Zhang et al. [63] following the structure design of Myrstad et al. [52] and Piermartini et al. [53]. They compared a mini-fixed bed reactor, a parallel straight microchannel reactor, and honeycomb fractal microreactor in the framework of olefin production in a HTFT process and concluded that the fractal configuration is better than the other concepts. Straight channels have been applied, e.g., by Cao et al. [64]. At a high gas hourly space velocity of 60,000 h^{-1}, they found a catalyst productivity of 2.1 g g^{-1} h^{-1} C_{2+} while still maintaining a methane selectivity less than 10%.

Loewert et al. [65] showed in their study that microstructured reactors from INERATEC GmbH can reach at least 2.1 g g^{-1} h^{-1} C_{5+} catalyst productivity and a record value of reactor space time yield of 1785 kg m^{-3} h^{-1} at isothermal conditions all over the reactor in pilot scale. These reactors are further equipped with a more complex heat removal microstructure allowing for optimized water evaporation with high efficiency. Catalyst deactivation was plotted in this study over 1000 h in a lab-scale experiment with near stable conversion in the end of the period. The run was performed at a constant temperature as high as 240 °C to show that the catalyst

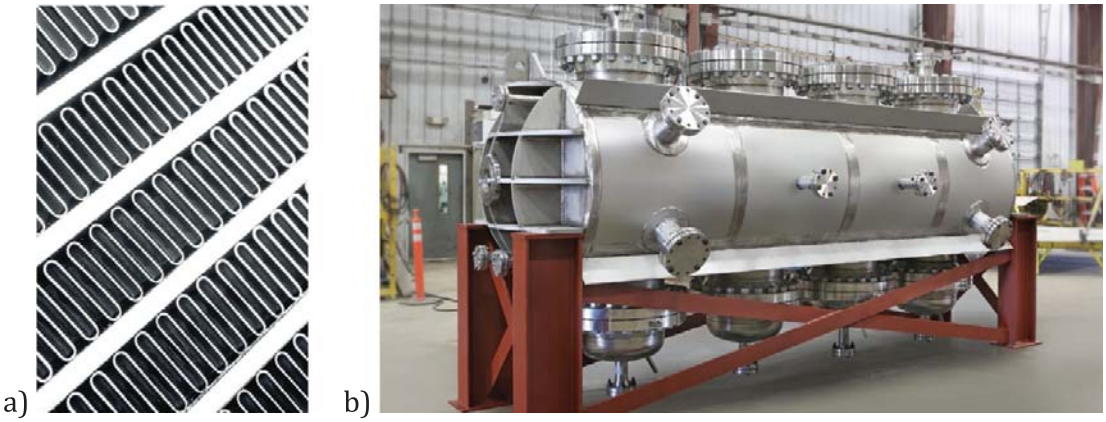

Fig. 6 a) Fin-strip-like structure of a Velocys reactor [67] and b) commercial scale 175 bpd reactor [68], https://futurefuels.blog/in-der-praxis/kerosin-aus-abfaellen/ (last accessed 08.09.2024)

can be operated for long time without pronounced deactivation under these harsh conditions.

In commercial scale straight channels are often reported, e.g., from the company Velocys Inc. (Fig. 6a)—these channels are adapted from fin-strip heat exchangers regarding costs' aspects. Water is evaporated in standard cross-flow to keep the temperature of the system under control. In the study by Steynberg et al. [66], the conversion drop over 60 days at around 70% per pass conversion of the commercial unit is shown. The average reactor temperature was manipulated to increase in the run from 205 to 210 °C with an accompanied methane selectivity increase by roughly 1% (absolute).

Regarding manufacture of microchannel systems, 3D printing has recently been proposed as well, e.g., from Mohammad et al. [69]. Nevertheless, this study is still quite preliminary, as they used a self-prepared catalyst made from silica with a methane selectivity of 14%. Under these conditions, they showed that single and parallel reactor arrangements yield the same product. From industrial point of view, production of the reactor with 3D printing still requires improvement regarding achievable reactor size. In addition, it needs to be considered that the pressure requirement of FT synthesis is an issue of wall thickness for 3D printing.

The developments toward commercial application of microchannel or microstructure technology are more and more increasing. Fischer-Tropsch microchannel reactors are discussed in the framework of BtL from Velocys with their scale-up of individual reactor units from 125 up to 175 barrels per day (bpd) (Fig. 6b). Jung et al. [68] and Na et al. [70] with the Korea Gas Corporation recently demonstrated an up-scale to a 1 bpd unit. Their approach is similar to the Velocys reactor concept (Fig. 7). They could show that the operation of the microreactor prevented thermal runaway in contrast to a fixed bed, which was more complex to operate [70].

INERATEC has also reported about the commercial scale reactors in a recent study [71]. Following the pilot scale results [65], they showed 2 bpd reactors (Fig. 8) and their current scale-up to 1.25 MW units (based on electrical power for hydrogen production capacity). These units come along with also rWGS reactors, which are

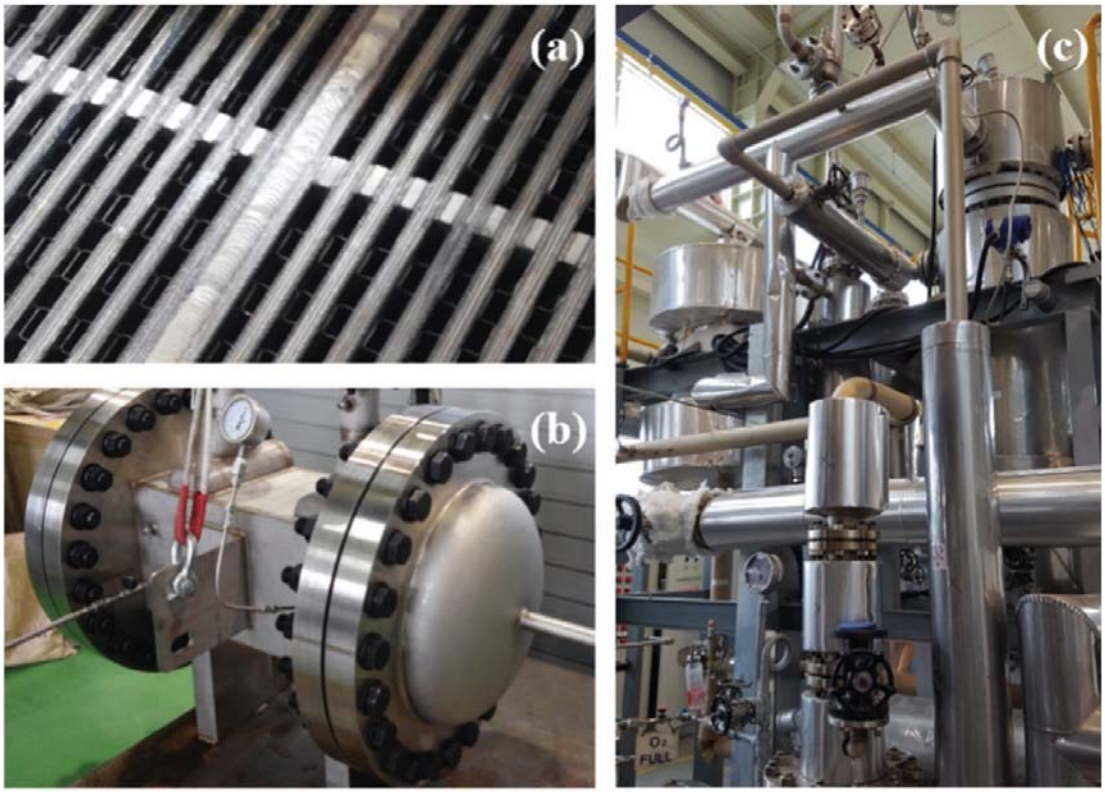

Fig. 7 Reactor module of 1 bpd dimension [68]: **a** internal structure with fin-strip-like structure, **b** reactor, and **c** setup for testing (bpd: barrel per day)

also made from microstructure technology, and a complete process starting from CO_2 and hydrogen for PtL applications.

3.2.2 Monolithic and Loop Reactors

Monolithic reactors have been proposed frequently as possible solution in the form of a loop reactor. One of the first publications on the use of monoliths for FT is from Mesheryakov et al. [72]. They showed that thin catalyst sheets permit to avoid intradiffusional resistance. They concluded that the small geometry-equivalent sizes of the gas bubbles and the high specific surface of the catalyst packing provide the intense gas-liquid-solid mass transfer. Further advantages were discussed from the point of low-pressure drop. Deugd et al. [73] have investigated this concept (Fig. 9) in depth from modeling point of view including the external recycle with heat removal which is necessary to achieve industrial relevant conversions per pass.

They compared the reactor volume to a study of the required size of a slurry bubble column from Maretto and Krishna [74] and came up with the conclusion that the monolithic reactor is smaller for an equal production capacity of 5,000 tons/day of middle distillates. The required slurry reactor volume is 4,410 m^3 divided into three vessels of 30 m height and 7 m diameter.

Fig. 8 Approved 2 bpd reactor module from INERATEC GmbH inside the skid of a 1 MW(el) PtL plant [71] (bpd: barrel per day)

Deugd et al. estimated a significantly smaller monolith reactor volume. Even though the internal heat removal and a lower temperature rise in case of the slurry bubble column, they conclude that plug flow behavior in the channels of the monolith reactor is a clear advantage enabling a higher productivity compared to the slurry bubble column. They also propose that the advantage of the monolith system is the fixed catalyst eliminating problems of catalyst attrition and separation. Attrition is, however, to some extent negligible over deactivation due to poisonous trace components which could occur in the context of PtL. As such, operation requires the exchange of the monoliths, which could be a considerable cost disadvantage.

Figure 10 shows the coated monolith from the work of Güttel [75]. He also pointed out that, although the preparation is reproducible, differences in the distribution of the active material were observed against the normal catalyst powder preparation. This is a general issue frequently observed for coatings in microstructured reactors as well. Further, catalyst accumulation in the corners of the quadratic channels needs to be avoided since it affects the diffusion distance. If the coatings are thick, the selectivity can be manipulated as reported also from larger particles [76].

During catalytic measurements in the catalytic setup, the group found that internal and external mass transfer affect the reaction rate and methane selectivity. External mass transfer constrains the reaction rate when the catalyst is coated. It is explained by the small relative velocity between catalyst particles and surrounding liquid, since the catalyst particles are entrained in the liquid. However, it was confirmed that the

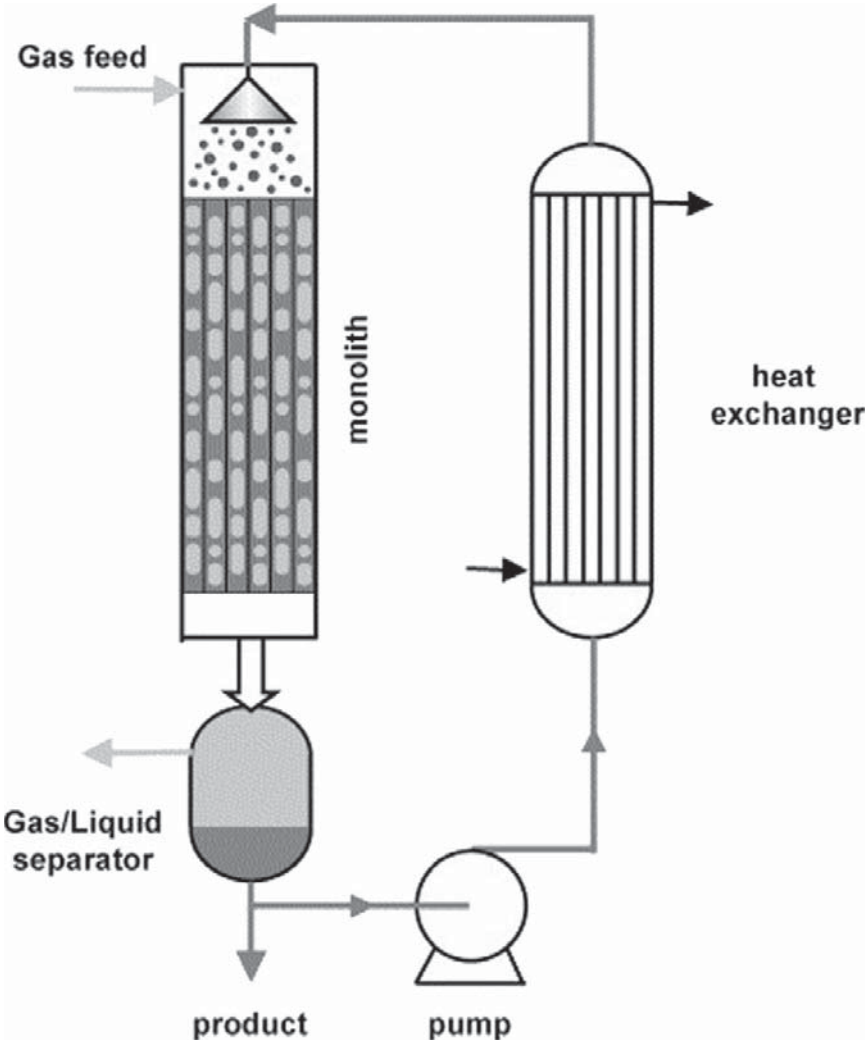

Fig. 9 Schematic drawing of the monolithic loop reactor with liquid recycle [73]

option of catalyst-filled channels is a preferred over coated channels by comparing the latter approach with a standard fixed bed. The enhancement in reaction rate is most probably caused by the advantageous external mass transfer characteristics of the monolithic catalyst in slug flow regime.

Merino et al. [77] investigated the effect of catalyst layer macroporosity in high-thermal-conductive monolithic Fischer-Tropsch catalysts with cobalt (Co) as active site. They applied coatings with one pore distribution centered at ~ 6 nm and another consisting of a meso-macroporous support with a wider pore size distribution centered at mesopores of ~10 nm and a significant macropore ($d_{\text{pore}} = 50$–$1{,}000$ nm) contribution. At iso-conversion and isothermal conditions with negligible differences of cobalt loading, it was concluded that the reduced methane selectivity and higher C_{5+} selectivity in the microporous coating arises from less diffusion resistance even though the coating was thicker due to lower density. This finding is obviously like the study of layer thickness in microchannels [57, 58] and special care must be taken when designing the catalyst layer.

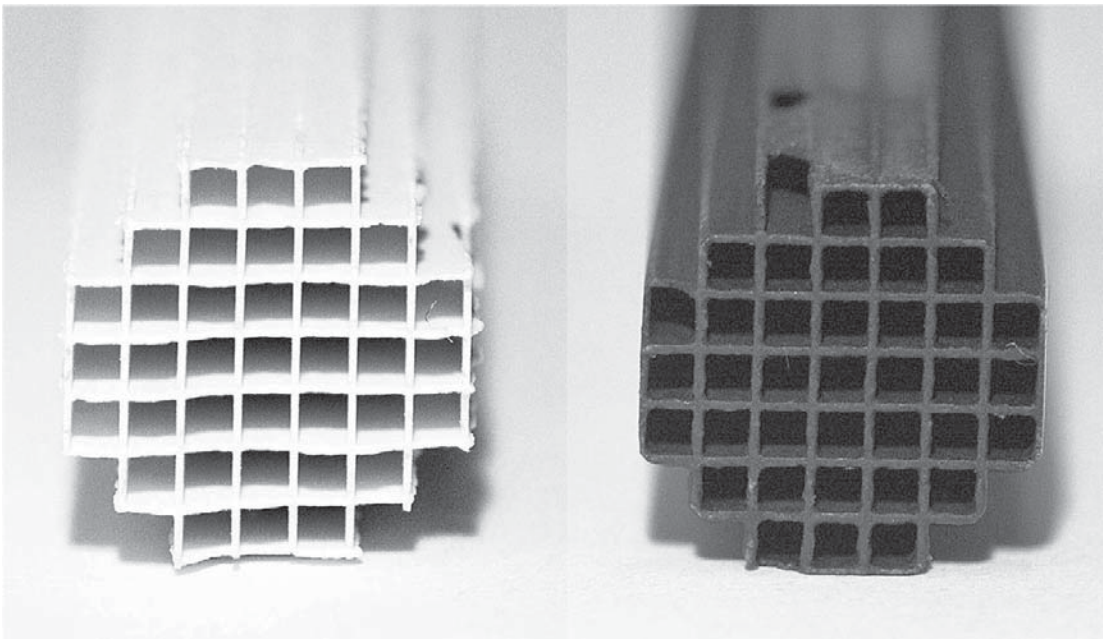

Fig. 10 Photograph of an uncoated (left) and coated (right) honeycomb monolith [75]

Visconti et al. [78] studied the importance of the thermal conductivity of the applied monoliths. They found by modeling that heat conduction in an aluminum support of the catalyst can be exploited to effectively remove the heat generated by the strongly exothermic FT reaction. Flat axial and radial temperature profiles along the catalytic bed, according to their conclusion, can guarantee an excellent temperature control without the need of recycling a fraction of the liquid reaction products, neither during reactor startup nor in continuous operation. Thus, monoliths may not only be used in the framework of loop reactors. In a later study [79], they tested 3D-printed highly conductive periodic open cellular structures (POCS). Arguing with the requirement of scaling down the conventional packed-bed multi-tubular reactors to modular compact units in the framework of biomass-to-liquid (BtL) and power-to-liquid (PtL) applications, their results seem promising. They indicated that the adoption of a conductive POCS enables to operate an FT reactor in isothermal conditions even under very severe conditions of high CO conversions corresponding to high volumetric heat duties. Comparing their results with open cell foams (Fig. 11), they found improved heat transfer coefficients for the ordered structure of the POCS over foams. Further, they highlighted that packing of the POCS structure with catalyst particles is also boosting the overall space–time yield compared to coated POCS or foams. These results are indicative for other approaches to intensify standard fixed bed or slurry bed reactors as discussed in the following section.

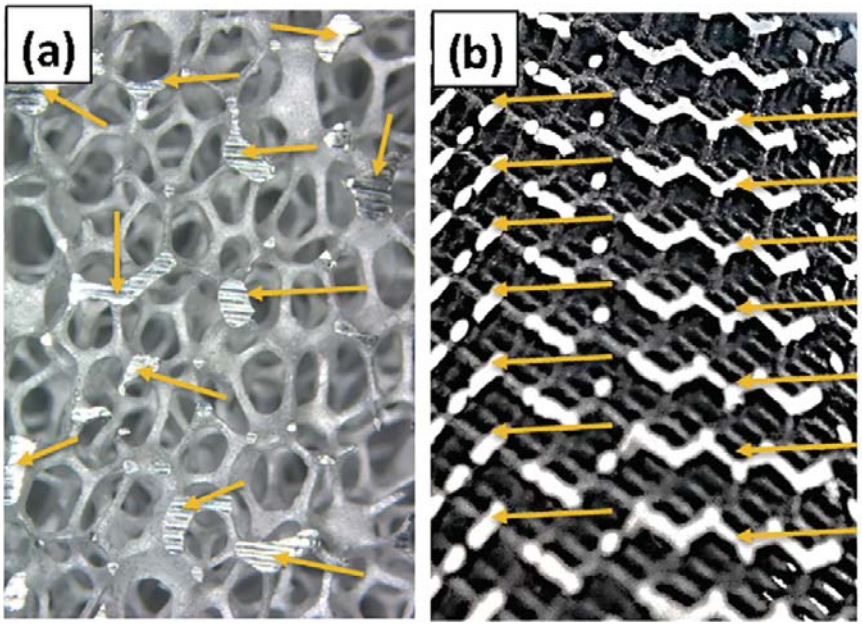

Fig. 11 **a** Open cell foam and **b** periodic open cellular structure applied in the study by Fratalocchi et al. [79]

3.2.3 Intensification in Traditional Reactors

Fixed bed bundle-type reactors are often used for low-temperature FT synthesis. As indicated in the previous section there are some attempts to intensify this type of reactor further. Johnson Matthey and BP recently introduced their CANS catalyst carrier system for Co-based FT synthesis [80]. The system works according to the following description:

1. Syngas from the catalyst carrier body above is guided downwards a porous central channel A (see Fig. 12).
2. The syngas then flows radially through the catalyst bed where heat is evolved (Fig. 12, arrows B).
3. The gas exits via a porous outer wall, flowing toward the top inner side of the catalyst carrier body (Fig. 12, arrows C).
4. Cooling occurs as the gas flows down the narrow annulus between the body and inside wall of the tube, through the transference of heat to boiling water on the shell side (Fig. 12, arrows D).
5. A seal prevents gas bypassing of the next catalyst carrier body, and the gas then enters the body below with the process then repeated (Fig. 12, arrows E).

According to the authors, a wider tube with improved heat transfer through the annular gas is feasible. In addition, higher gas velocities are said to be possible due to the short path through the catalyst bed. Smaller catalyst particles are also envisaged to be used through the short catalyst bed length. Nevertheless, from the point of flow directions, this concept seems to introduce some hurdles for Co-based FT synthesis as the liquid formed is entrapped in the core of the system until it is flooded.

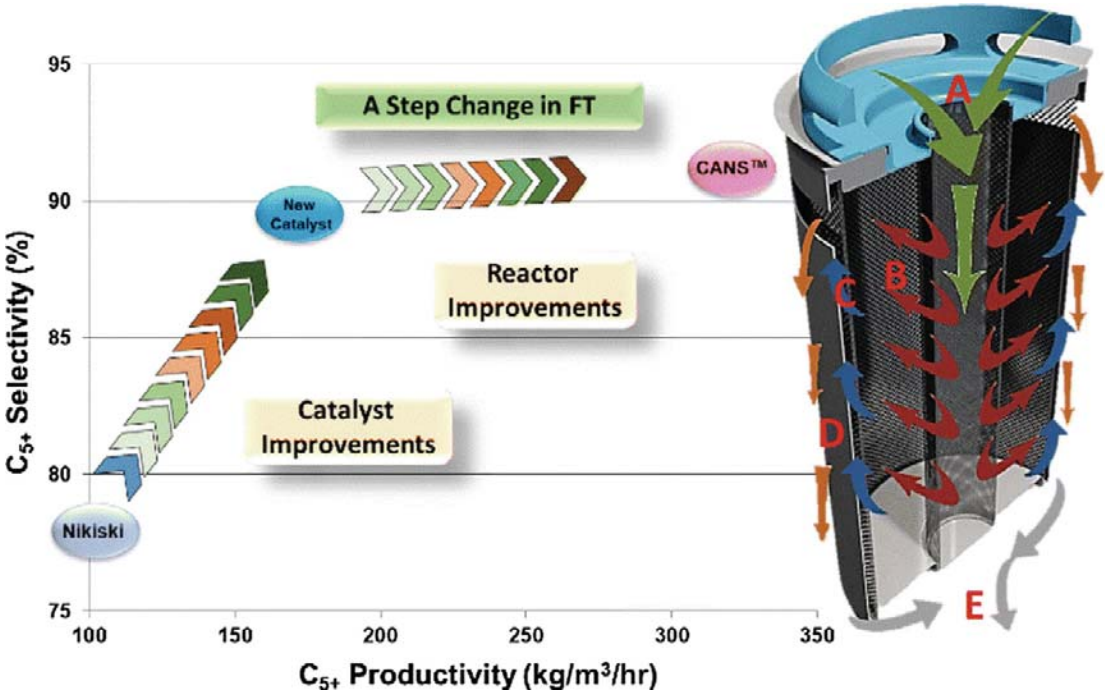

Fig. 12 CANS catalyst carrier system from Johnson Matthey and BP [80]

Another approach is based on improved heat conductivity on the catalyst level. Asalieva et al. [81] tested thermally conductive additive (Al, Cu, or Zn metal powder) for cobalt-based catalyst.

Pangarkar et al. [82] did an early evaluation of the concept of implementation of packings into the fixed bed tube. Structured packings such as open cell flow structures (OCFS) and closed cell flow structures (CCFS), but also knitted wires and open cell aluminum foams were investigated. They found that the heat transfer coefficient in regular flow structures is superior to that of randomly ordered structures, which can be explained by the shorter heat transfer path. The randomly ordered catalyst packing is even worse in heat transfer due to the almost missing solid heat conduction.

Among studies on integrating foams [83], a recent study on packed-POCS with skin was published by Fratalocchi et al. [84]. The so-called POCS with skin (Fig. 13) is characterized by a surrounding tube thermally connected with the internal diamond structure of the POCS through the printing process. According to the authors, this resulted in an increase of the contact to the reactor tube, which enabled heat transfer from the POCS to skin and the wall to be governed by heat conduction rather than convective heat transfer. Thus, a further improvement in this technology is envisaged.

Hooshyar et al. [85] modeled the improvement of structured packings in fixed bed arrangements as well as in slurry bubble columns. They found out that the insert is eligible for both reactor types. In the slurry bubble column backmixing is also reduced, which could lead to an improvement in reactor productivity of 20% in the slurry bubble column and up to 40% in the fixed bed reactor.

Frost et al. [86] showed the development of a compact Fischer-Tropsch reactor based on heat conductive internals shown in Fig. 14a and the pilot scale system in

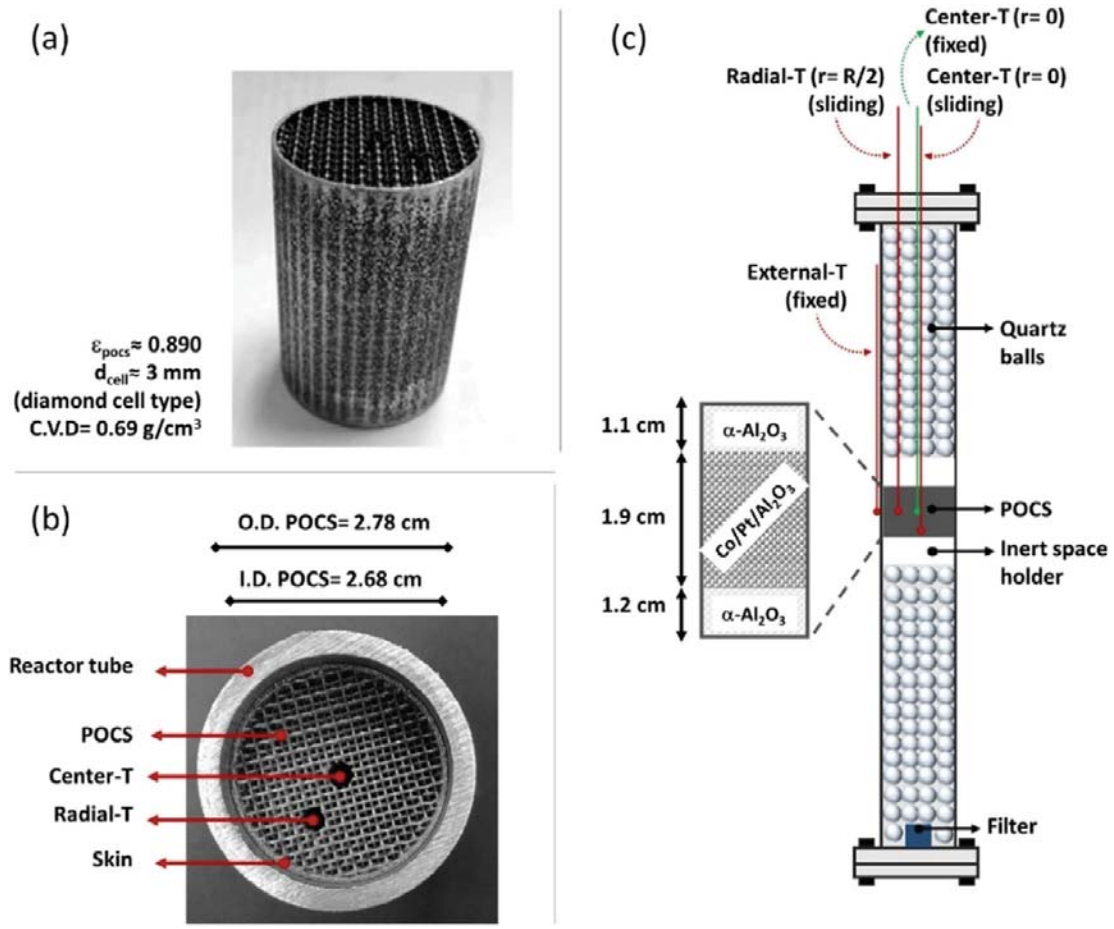

Fig. 13 (a) and (b) side and top view images of POCS and (**c**) schematic diagram of a reactor tube with a single POCS insert packed with catalyst pellets and α-Al_2O_3 [84] (POCS: periodic open cellular structures)

Fig. 14b. Unfortunately, no later reports are available of the Ceramatec Inc. system. Nevertheless, recently a study on a methodological study on the reactor internals by Barrera et al. [87] with coauthors of Frost was published.

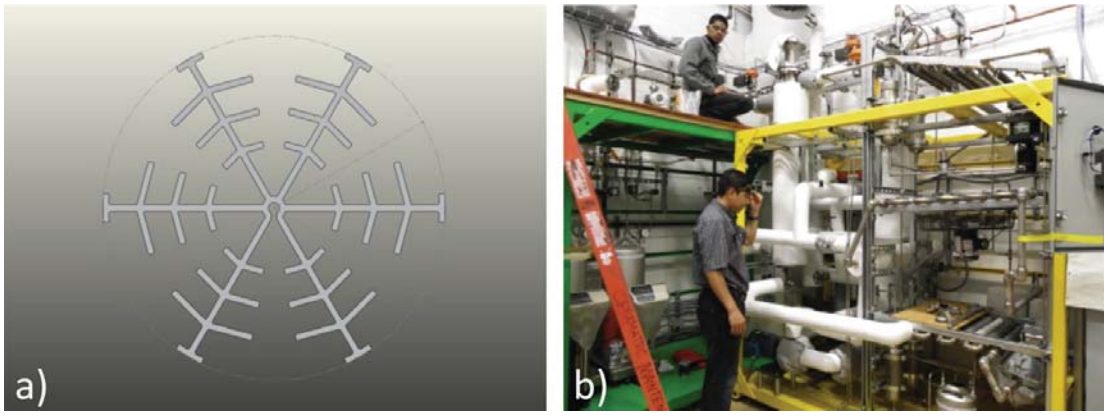

Fig. 14 **a** Internal reactor insert for thermal transfer and **b** pilot scale FT reactor system [86]

Kapteijn and Moulijn [88] also gave a recent more general perspective for the structured catalysts and reactors from the viewpoint of heat conductive inserts, which provides a more detailed overview on the aforementioned studies.

A completely other approach to improve the multi-tubular fixed bed reactor is the use of phase change materials (PCM) to manage temperature control. Odunsi et al. [89] suggested that the PCM material should be located at the outer perimeter of the individual tubes. The delay in temperature rise due to phase transition by the PCM, according to their calculations, could keep the catalyst bed in a narrow temperature window. This technology is, however, not being exploited commercially, maybe because of the rough environmental conditions for the PCM material in the multi-component mixture of the FT synthesis.

Apart from the suggestion of cell structures for intensifying the slurry phase reactor [85], An et al. [90] also modeled an increasing reactor productivity with increasing number of internal tubes in the slurry phase. However, there is no experimental proof for these simulative results. Geng et al. [90, 91] wrapped up the approaches of agitated slurry reactors in a general perspective. These approaches could also be transferred to FT synthesis regarding process intensification. Agitation can help to improve hydrodynamics and mass transfer, i.e., superficial velocity increase between gas, liquid, and solid phase as well as less backmixing, higher gas holdup and associated higher interfacial surface area.

3.3 Other Means of Intensification

3.3.1 Supercritical FT

Supercritical operation conditions are often discussed as method to avoid mass transport limitation. A review from 2009 indicated that these conditions are promising although implementation of supercritical fluid in FT was still at laboratory scale at that time [92]. Supercritical condition for FT synthesis has been discussed by Mogalicherla et al. [93], but they found that supercritical conditions are not able to eliminate the diffusion effects in the pores of the catalyst. Larger particles will still be prone to a H_2/CO ratio shift due to different diffusion coefficients of H_2 and CO in the catalyst pores filled with hydrocarbons. This leads to enhanced chain termination.

In a follow-up simulation by Abusrafa et al. [94], the supercritical conditions were demonstrated to provide exceptional reduction in hot-spot formation with a maximum radial bed temperature variation < 15 K for a 4 inch internal diameter (ID) reactor bed as opposed to 800 K in an equivalent standard FT reactor bed. They concluded that process intensification by supercritical conditions can lead to up to 16-fold reduction in the number of tubes required to achieve a throughput equivalent to a conventional 1 inch ID reactor bed. Nevertheless, this technology has not been scaled yet to any pilot plant to our knowledge. This is most probably a matter of operational costs for implementation of the supercritical conditions and dominates over capital expenditure for the reactor size.

3.3.2 Integrated Upgrading

Tandem catalysis for FT and hydrocracking has also been proposed to enhance product selectivity and reaction rate by avoiding the accumulation of long-chain hydrocarbons in the catalyst bed [95, 96]. Addition of ZSM5 in a catalyst mixture [97], such as a combined coating on channel walls [98] or a core–shell structure, has often been applied, e.g., Refs. [99, 100].

Different schemes of integration of hydrocracking into the process of rWGS and FTS have been investigated by Kirsch et al. [101]. The authors suggest direct coupling of FTS and HC as otherwise intermediate product separation improves the liquid fuel yield just by a few percent based on modeling. Arguing that compact processes are particularly important for flexible small-scale plants for decentralized application regarding the energy transition, it is believed to be advantageous to directly convert the formed wax in situ. In a follow-up study, advanced process design of a special bifunctional catalyst bed is proposed (Fig. 15) [102]. While hydrocracking in the presence of CO can lead to secondary cracking and is largely prevented by a liquid film entrapping the hydrocracking catalyst, either a gradient with increasing hydrocracking catalyst along the catalyst bed or a sequential bed with a second stage having a low FT catalyst mass contribution is proposed. Nevertheless, Brosius [103] recently explored the possibility of ambient pressure hydrocracking on a Pt/HY catalyst (a catalyst where platinum (Pt) particles are dispersed or supported on a HY zeolite material), which allows to reach much higher yields of liquids. This may be more advantageous also in the field of smaller-scale plants.

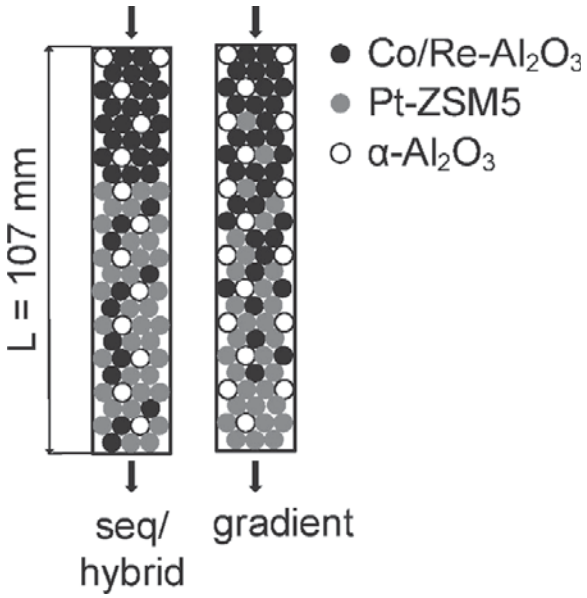

Fig. 15 Distribution of FT and hydrocracking catalyst over the catalyst bed for avoiding secondary cracking in the presence of CO: in the gradient configuration the amount of FT catalyst is linearly decreasing, whereas the amount of HC catalyst is linearly increasing. The catalysts are diluted with inert α—Al_2O_3 [102]

3.3.3 Sequential Reactors

A sequence of FT reactors with intermediate removal of products and the formed byproduct of water is frequently discussed in patents [104] and literature [105, 106]. Common sense is that the per pass conversion can be limited to a level where hot-spot formation is under control, inert gases do not accumulate, and water partial pressure increase is avoided. In this way, a critical H_2O/H_2 ratio for oxidation of the cobalt or iron catalyst is prevented. Pandey et al. [105, 106] recently investigated the optimal reaction trajectory for a three-stage process and found that an under-stoichiometric H_2/CO feed with maximum possible total CO conversion (93.6%) and operation at a conversion per pass of 60% is an optimal strategy for once-through three-stage FT synthesis, which is generally applicable for the FTS over a cobalt catalyst.

In the framework of power-to-liquid, however, the conversion in the FT stage may not be as relevant as in the gas-to-liquid or biomass-to-liquid application. Typically, low inert composition is intended via CO_2 and H_2 in the PtL case. Thus, a recycling of unreacted gas over the rWGS stage is feasible and recovers the already existent CO and H_2 in the process while methane can be converted via in situ reforming on the catalyst.

3.4 Process Integration of rWGS and FT

It has already been discovered in the 1930s during early Fischer-Tropsch research in Germany that carbon dioxide (CO_2) can, similarly to carbon monoxide (CO), be converted to higher hydrocarbons [107, 108] using alkalized iron, cobalt, or ruthenium catalysts. Presumably due to the lack of commercial relevance, a small number of studies or patents were published up to the mid-1990s [109, 110, 110–114]. Along with the global awareness for the effects of greenhouse gas (GHG) emissions, a growing interest in the utilization of CO_2 as a carbon source developed in the last decades [115, 116]. Especially worth mentioning are the early works at the Korea Research Institute of Chemical Technology (KRICT), which are summarized in a review of Sai Prasad et al. [117]. The current research is mainly focused on the development of suitable catalysts and is summarized in several detailed reviews [115, 116, 118, 119, 120, 121].

3.4.1 Reaction Network

As the current research mainly focuses on iron-based catalysts (see below), the focus on any reaction characteristics will be put on these catalysts. It seems to be consensus that the reaction proceeds via two consecutive reactions: CO_2 is first reduced to CO via the reverse water–gas shift (RWGS, Eq. 8), which is then converted to a hydrocarbon mixture through a conventional Fischer-Tropsch (FT) synthesis [122–125]. Iron-based catalysts are especially suitable for this process as they catalyze

both reactions. Under reaction conditions, several iron oxide and carbide phases coexist [126]. In this mixture, the rWGS activity is mainly ascribed to Fe_3O_4 while the FTS activity is ascribed to χ-Fe_5C_2 (Hägg carbide) [124, 125]. A direct formation pathway of hydrocarbons from CO_2 may exist to some extent but is likely negligible compared to the indirect pathway [122].

$$CO_2 + H_2 \leftrightarrow CO + H_2O \quad \Delta_R H^0 = 41 \ \text{kJ mol}^{-1} \tag{8}$$

The overall balance is given by Eq. 9. One should note the large amount of water that is formed in the reaction, being the main product.

$$CO_2 + 2H_2 \rightarrow (CH_2) + 2H_2O \quad \Delta_R H^0 = -122 \,\text{kJ mol}^{-1} \tag{9}$$

The large amount of water that is formed in the reaction is a main challenge for a realization of the process as it does not only strongly inhibit the reaction [127, 128, 129], but may also lead to catalyst degradation via oxidation at high water partial pressures [128, 130, 131].

3.4.2 Proposed Catalysts

Iron-Based Catalysts

Iron-based catalysts have been widely applied for the CO_2-FTS (process variant #2, Table 1) due to their activity for both, rWGS and FTS, and their remarkable flexibility regarding the feed gas composition. Unlike cobalt, iron catalysts do not require high CO partial pressures to establish a chain growth regime and can yield a product spectrum similar to the traditional FTS when using H_2/CO_2 feed gas mixtures [132]. CO that is formed in situ via the rWGS is sufficient to sustain chain growth. The catalysts usually require a stronger alkali promotion [133]. Under typical operating conditions of 300 °C, the product spectrum does usually resemble a high-temperature FTS, with short-chain 1-alkenes being the main product [128].

Iron-based catalysts may be divided into three categories depending on the preparation pathway: precipitated, supported, and fused catalysts. Iron (Fe) bulk catalysts prepared via precipitation have been applied for decades in the low-temperature FTS and have been demonstrated to be also applicable for the CO_2-FTS [122, 126, 132, 134]. Supported iron catalysts have hardly been applied for the traditional FTS due to the poor reducibility and lowered promoter effectiveness [135, 136]. For the CO_2-FTS, however, potassium-promoted alumina-supported iron catalysts have been adopted in several studies, which demonstrated a remarkable activity and selectivity [137]. They still require a high reduction temperature (>400 °C) and high potassium content. For the high-temperature FTS fused iron catalysts are applied commercially by Sasol [135]. This type of catalyst has gained limited attention for the CO_2-FTS so far [138].

Among promoters, the importance of alkaline promoters (potassium (K) [133, 137, 139, 140, 141, 142] or sodium (Na) [143, 144, 145, 146, 147]) is usually highlighted to tune the catalyst performance. Alkali metals improve the adsorption of CO_2 and CO, increase the selectivity to alkenes, and drive the product spectrum to long-chain hydrocarbons [116, 118]. An approach that has gained considerable attention in the last years is the combination of an iron-based catalyst with a zeolite (usually H-ZSM-5) to directly convert short-chain alkenes to aromatic components [123, 148, 149]. This route may be of particular interest for gasoline applications.

Cobalt and Ruthenium

Cobalt-based catalysts for the traditional FTS are usually supported catalysts using a porous carrier (alumina, silica, titania, etc.) with a noble metal promotion (platinum (Pt), rhodium (Rh), rhenium (Re)) [135]. These catalysts are not applicable for the CO_2-FTS as they require a high CO partial pressure to establish a chain growth regime and thus mainly act as methanation catalysts when exposed to CO_2-H_2 mixtures [124, 132]. However, alkali promotion was shown to suppress methane formation and enhance the selectivity to long-chain hydrocarbons [150, 151, 152]. Hence, it may also be possible to employ Co-based catalysts for the CO_2-FTS upon further development.

Ruthenium (Ru)-based catalysts are well known for their high activity and selectivity to long-chain hydrocarbons in the traditional FTS, but are not applied commercially due to the high costs and poor availability of the noble metal [135]. Unpromoted Ru catalysts mainly catalyze methane formation under the conditions of CO_2-FTS [107, 111]. Like for cobalt, however, alkali promotion showed to suppress methane formation and to improve the selectivity to higher hydrocarbons [107]. For the same reasons as for the CO-FTS, it is unlikely that Ru will become a relevant catalyst candidate for the CO_2-FTS.

3.4.3 Process Considerations

Unlike the two-stage rWGS/FTS process, there has been very limited work beyond lab scale for the CO_2-FTS. The main challenges have been identified and are outlined below.

Implications of Water Formation on Process Concept

A key part of a direct-FT scale-up concept is the effective removal of water vapor from the reaction mixture to overcome the limitation of a small conversion per pass. In a patent from 1954, Kölbel and Ackermann proposed two possible concepts: multiple reactors in series with intermediate condensation or a recycle reactor with continuous product condensation [109].

Both concepts have been adopted in more recent studies: Landau et al. achieved a CO_2 conversion of up to 89% in a bench-scale setup with three reactors in series with intermediate condensation and Guo et al. demonstrated a conversion of almost 70% in a two-stage reactor system. Choi et al. [153] realized the recycle reactor concept and achieved a CO_2 conversion of up to 88%. The only study at pilot scale has been reported by Willauer et al. [154] who achieved up to 69% CO_2 conversion under recycle conditions. Along with the conventional process concepts, Rohde et al. proposed a membrane reactor concept which allowed an in situ removal of water vapor from the reaction mixture [155]. This concept does still further development of membrane materials, though [156].

Reactor Design

So far, experimental studies have been reported almost exclusively in fixed bed reactors. However, the typically observed limited long-term stability (< 1 year) of iron-based FTS catalysts [135] may favor other reactor concepts for a large-scale application. Fluidized bed or slurry reactors are established reactor concepts for the conventional FTS and would allow for online catalyst replacement [157]. Kim et al. [158] studied different reactor concepts for the CO_2-FTS and demonstrated the applicability of fluidized bed or slurry reactors.

Brübach et al. [130, 159] studied the process on supported iron in two different scales of a tubular reactor. In the second part of their study, a large 1 inch tubular reactor scale was operated under recycling conditions. With a detailed kinetic model, they were able to predict the reactant consumption, as well as the hydrocarbon distribution, reliably within the experimental range studied (10 bar; 280–320 °C; 900–120,000 $mL_N h^{-1} g^{-1}$; and H_2/CO_2 molar inlet ratios of 2–4). High conversions up to 80% demonstrated the applicability of the process concept. Fractions of individual hydrocarbon classes (1-alkenes, n-alkanes, and iso-alkenes) were accounted in their model with chain-length-dependent kinetic parameters for branching and dissociative desorption. They found that hydrogenation is the main reaction involved while recycling short-chain olefins into the reactor. No chain growth occurred through re-adsorption. Further, hot-spots occurred in the larger reactor which required catalyst dilution, and thus, more advanced reactor concepts could be helpful here as well. Catalyst stability and potential coke formation could, nevertheless, be crucial.

Syncrude Refining

The refining of the synthetic crude (syncrude) is the final step for fuel applications. Due to many similarities to the cobalt-based high-temperature FTS, the refining may be conducted in a similar manner [128, 160]. When aiming for middle distillates (kerosene and diesel), oligomerization of alkenes would be a key refining step [161, 162]. Oligomerization on aluminosilicates like hydrogenated Zeolite Socony Mobil-5 (H-ZSM-5), amorphous silica-alumina (ASA), or solid phosphoric acids

(SPA) may be appropriate technologies [163]. The selectivity to oxygenate (mainly alcohols, carbonyls, and carboxylic acids) is neglected in many studies but presents a considerable part of the product fraction for cobalt-based catalysts and should be considered for the refining strategy [160, 163, 164]. Hydro-processing steps are especially susceptible to the presence of oxygenates and must be designed appropriately [164]. Lower molecular weight oxygenates are preferably dissolved in the aqueous phase. For a high carbon efficiency, recovery of hydrocarbons from the aqueous phase should be considered [165].

4 The Aspect of Transient Operation in PtL

In the framework of power-to-liquids, the production of the powerfuels based on renewable energies as well as carbon dioxide, e.g., from ambient air, biogenic sources, or unavoidable fossil point sources, is feasible. The entire supply chain is then CO_2 neutral or at least no additional CO_2 is emitted, respectively. The intermittency of renewable power, nevertheless, imposes a serious problem for continuously running a PtL plant. The peak power generation must be enlarged greatly or either certain/large volumes of hydrogen storage are needed, or the synthesis plants must also run in transient modes.

Pfeifer et al. [166] have investigated the operation of INERATEC plants regarding electricity production from 80% photovoltaics and 20% wind energy for the German Federal State of Baden Württemberg on the basis of varying peak power versus electrolyzer and synthesis plant size in dependence on the load flexibility of the synthesis plant. They found that high renewable energy and synthesis plant utilization degree of above 80% can be reached with the turndown ratio of their plants as high as 83%; valid for a storage capacity of hydrogen of 10 h for the lowest load point of the synthesis plant. Figure 16 shows plots of time-related renewable power and load state of the synthesis. It shows that of course a certain larger peak power must be installed, while available power is transferred with above 80% utilization through small hydrogen storage capacity into fuel. Further, the hydrogen buffer volume can be reduced by operating the plants in transient mode feasible through modularity. Although no information on the capital expenditure saving is available, the concept should be followed for safety reasons.

Several authors have investigated the Fischer-Tropsch reaction under transient conditions [167, 168, 169, 170, 171, 172, 173] in the framework of varying load. Some research is also summarized in a review [174]. There is common sense that Fischer-Tropsch intrinsic reactions on cobalt, in contrast to iron where phase changes can occur even after days, are fast enough to be described by stationary kinetics [167, 168, 169, 170, 171, 172], even for highly transient conditions in the minute scale through monolithic or microstructured reactors [169, 171, 172].

De Swart and Krishna [175] enabled simulation of slurry bubble columns to better design and stabilize hydrodynamics of these reactor types in transient conditions. Nevertheless, Loewert et al. [171] demonstrated experimentally, that plants with

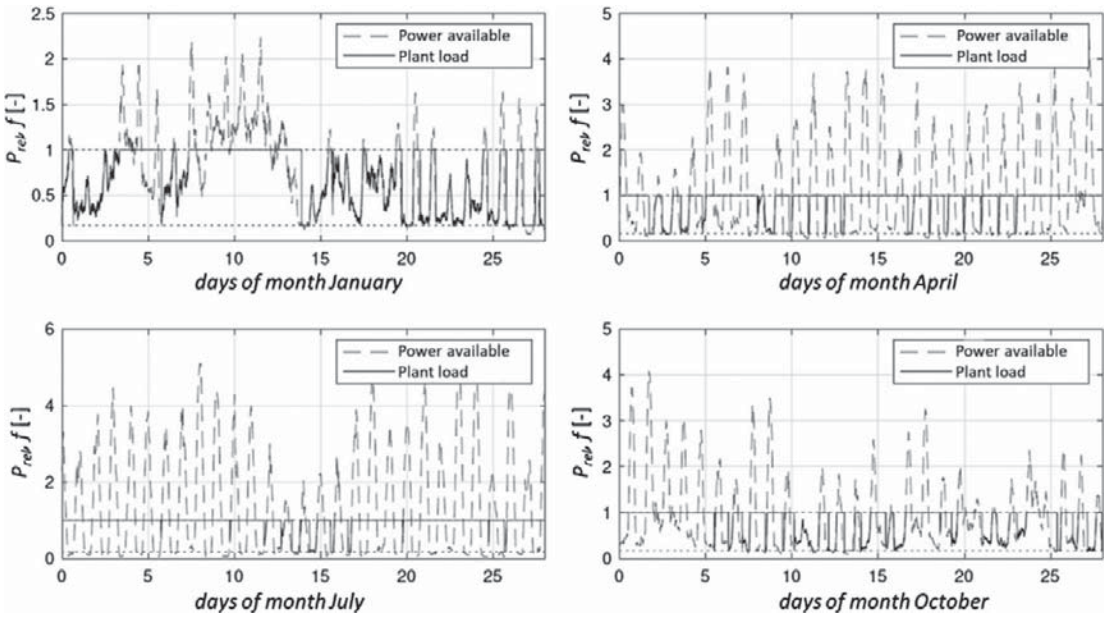

Fig. 16 Relative electric power and load of the fuel plant for selected months (for the German Federal State of Baden Württemberg) at a fuel plant capacity $F_{max} = 1$, a tank size for peak power $t_{peak} = 10$ h, and a wind/photovoltaic (PV) ratio of 20:80. Minimum tank capacity $t_{min} = 1.3$ h [166]

microstructured reactors can be easily manipulated regarding the process conditions during changing loads on day and even at single minute scale. They applied a real photovoltaics (PV) profile to a reactor assuming instantaneous conversion via electrolysis. They could show that manipulation of the reactor temperature by changing the water evaporation conditions on the cooling side to keep the conversion on a high level of 65% the volumetric content of formed methane from FT was less varying over the day profile and thus advantageous over keeping the reactor temperature constant (Fig. 17). Only near isothermal operation would be feasible in slurry due to the high-thermal masses of accompanied liquid.

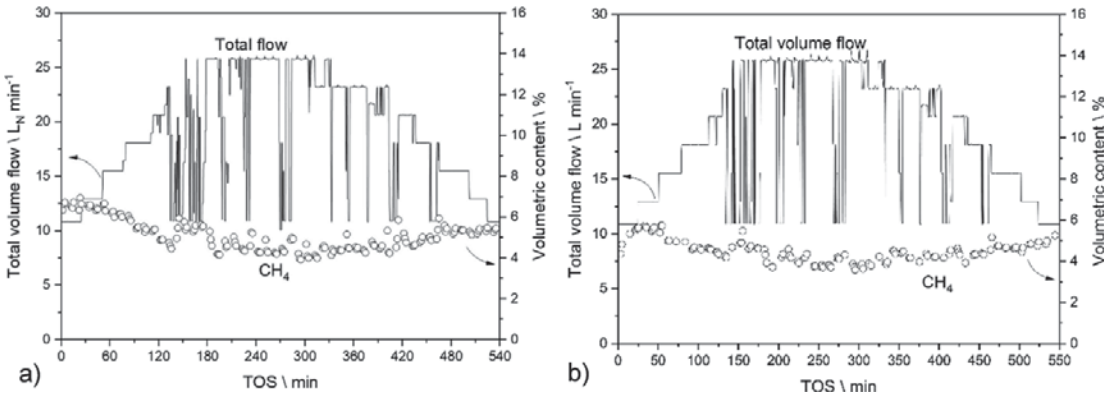

Fig. 17 Flow variation (constant H_2/CO ratio) according to the photovoltaic (PV) power and the resulting variation in methane volumetric content at **a** almost constant reactor temperature and **b** almost constant conversion of around 65% through reactor temperature manipulation [171]

In further studies by Pfeifer et al. [71], it is also shown that the microstructured reactors are controllable in serial and parallel operation also under transient conditions. They also concluded that start-stop can be performed with multiple reactors leading to high flexibilities regarding load so that, e.g., 83% of turndown ratio [166] seems feasible.

5 Comparison and Conclusion

In the context of integrating and utilizing powerfuels, particularly hydrocarbon Power-to-Liquid drop-in fuels like kerosene and diesel, the Fischer-Tropsch synthesis has emerged as a central technology and pathway in recent years. To rapidly deploy this technology at scale in the upcoming years and decades, besides the broader techno-economic and environmental aspects, understanding exact process conditions and specifications is equally vital. This includes in-depth analyses of aspects like catalyst utilization, reactor technologies, and approaches to effectively combine different sub-technologies and processes (e.g., electrolysis technologies, carbon dioxide activation, and FTS) as well as the aspect of intermittent feed and most suitable plant size at the point of use within an overall FTS pathway.

However, only a few comparative studies or reviews are available [51, 176, 177, 178] comparing reactor technologies and/or aspects in process intensification for Fischer-Tropsch synthesis. While Holmen et al. [178] compare different structured reactors and Venvik et al. [177] provide a review over microchannel reactors for FT, Saeidi et al. [176] also consider traditional reactors with internals. One of the most recent studies by Kee et al. [51] compares slurry, fixed bed, and microchannel reactors not only for FT but also for reforming and oxidative methane coupling. Therefore, this chapter aims to provide a concise overview of the diverse approaches for process intensification in FT, while also addressing the different aspects required for powerfuels on a process level. Such are, to name a few: CO_2 activation, space time yield, catalyst stability, and regeneration, as well as intermittent loads.

In light of the content and study results presented here, it seems that especially microstructured or monolithic and POCS are a good alternative to traditional FT reactor systems. While modularity is gaining importance for fast roll-out of the PtL technology and is best suited to address local availability of CO_2 and power, these technologies are just on the road. Giving an example, INERATEC's pre-assembled containerized or skid-mounted systems are already on the market as integrated rWGS and FT process in 1 MW industrial pilot and a scale of up to 10 MW (Fig. 18) shall start operation in 2024 at the Frankfurt Hoechst site [179].

Other attempts in this area to mention are, e.g., the strategic alliance of Sasol EcoFT and Haldor Topsoe for FT and rWGS, respectively. Combined rWGS and FT in a single reactor are followed from, e.g., AirCompany [180, 181], Sasol [182], to name just a few. Hence, the future will basically show if all these concepts will come alive.

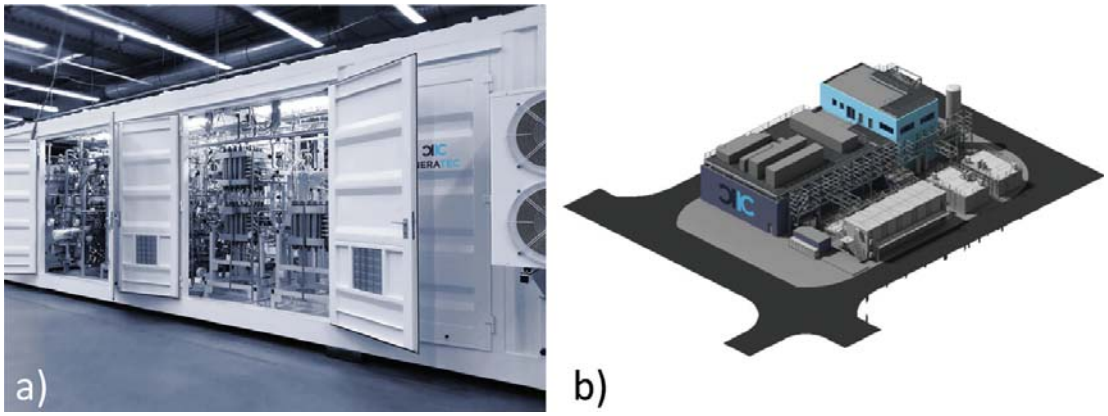

Fig. 18 **a** 1 MW industrial pilot and **b** concept of up to 10 MW plant for the Frankfurt Hoechst site [source: INERATEC GmbH]

In general, conventional cobalt-based as well as iron-based FT utilizing carbon monoxide are already approved for the production of synthetic kerosene from FT syncrude in the respective ASTM regulations for aviation turbine fuels (ASTM D7566). Looking at the future demand of CO_2 neutral aviation fuels, it is anticipated that a significant portion will be in the form of PtL kerosene, especially in the medium to long terms. Thus, FT could be a good option to fulfill this kerosene demand. Process-wise FT-based PtL kerosene, could be produced from all the FT process variants presented in this chapter while only direct CO_2-FT is not yet approved by ASTM D7566. Thus, for CO_2 originating from ambient air or biomass, the processes with upfront CO_2 reduction to CO (e.g., by rWGS) are ahead in time regarding today's regulation. Very good combustion properties, for example regarding reduced soot emissions, have repeatedly been demonstrated [183]. Climate effects from the formation of condensate are reduced additionally [184]. These better combustion properties arise from the absence of aromatics.

Furthermore, ASTM regulations fit for blending of up to 50% of the hydrotreated FT product to specification-compliant conventional (fossil) jet fuel. For CO_2-based FT a respective ASTM certification is still required, although, this could be relatively easily solved due to similar product quality compared to the HTFT process. Furthermore, it can be concluded that even with a higher demand for upgrading steps which is possible only in large installations, this route could play a role in the future. Nevertheless, cobalt-based FT processes might be the choice for distributed energy availability also in the smaller scale, i.e., in remote energy supply.

References

1. Unruh D (2006) Fischer-Tropsch Synthese mit Synthesegasen aus Biomasse—Verbesserung der Kohlenstoffnutzung durch Anwendung eines Membranreaktors (Ph.D. thesis, Universität Frider-iciana Karlsruhe (TH))

2. Steynberg AP (2004) Introduction to Fischer-Tropsch technology. In: Steynberg AP, Dry ME (eds) Fischer-Tropsch Technology, vol 152. Elsevier, pp 1–63
3. Steynberg AP, Dry ME, Davis BH, Breman BB (2004) Fischer-Tropsch reactors. In: Steynberg AP, Dry ME (eds) Fischer-Tropsch technology, vol 152. Elsevier, pp 64–195
4. Xu J, Yang Y, Li Y-W (2013) Fischer-Tropsch synthesis process development: steps from fundamentals to industrial practices. Curr Opin Chem Eng 2:354–362
5. Xu J, Yang Y, Li Y-W (2015) Recent development in converting coal to clean fuels in China. Fuel 152:122–130
6. Guettel R, Kunz U, Turek T (2008) Reactors for Fischer-Tropsch synthesis. Chem Eng Technol 31:746–754
7. Fischer F, Tropsch H (1926) Über die direkte Synthese von Erdöl-Kohlenwasserstoffen bei gewöhnlichem Druck. (Zweite Mitteilung). Berichte der deutschen chemischen Gesellschaft 59:832–836
8. Dry ME (2004) FT catalysts. In: Steynberg AP, Dry ME (eds) Fischer-Tropsch technology, vol 152. Elsevier, pp 533–600
9. Schulz H (1999) Short history and present trends of Fischer-Tropsch synthesis. Appl Catal A Gen 186:3–12
10. Dry ME (1981) The Fischer-Tropsch synthesis. In: Anderson JR, Boudart M (eds) Catalysis: science and technology. Springer, pp 159–255
11. Dry ME (2004) Chemical concepts used for engineering purposes. In: Steynberg AP, Dry ME (eds) Fischer-Tropsch technology, vol 152. Elsevier, pp 196–257
12. Frohning CD et al (1977) Fischer-Tropsch synthesis. In: Falbe J (ed) Chemierohstoffe aus Kohle, Thieme, pp 219–299
13. Khodakov AY, Chu W, Fongarland P (2007) Advances in the development of novel cobalt Fischer-Tropsch catalysts for synthesis of long-chain hydrocarbons and clean fuels. Chem Rev 107:1692–1744
14. Anderson RB (1956) Catalysts for the Fischer-Tropsch synthesis. In: Emmett PH, Dixon JK (eds) Hydrocarbon synthesis, hydrogenation and cyclization, vol 4. Reinhold, pp 29–255
15. Oukaci R, Singleton AH, Goodwin JG Jr (1999) Comparison of patented Co F-T catalysts using fixed-bed and slurry bubble column reactors. Appl Catal A Gen 186:129–144
16. van de Loosdrecht J et al (2013) Fischer-Tropsch synthesis: catalysts and chemistry. In: Comprehensive inorganic chemistry II (second edition): from elements to applications, vol 7. Elsevier Ltd., pp 525–557
17. Vogel AP, van Dyk B, Saib AM (2015) GTL using efficient cobalt Fischer-Tropsch catalysts. Catal Today 259:323–330
18. van Steen E, Claeys M (2008) Fischer-Tropsch catalysts for the biomass-to-liquid (BTL)-process. Chem Eng Technol 31:655–666
19. Dry ME (2002) The Fischer-Tropsch process: 1950–2000. Catal Today 71:227–241
20. van der Laan GP, Beenackers AACM (1999) Kinetics and selectivity of the Fischer-Tropsch synthesis: a literature review. Catal Rev Sci Eng 41:255–318
21. Dry ME (1996) Practical and theoretical aspects of the catalytic Fischer-Tropsch process. Appl Catal A Gen 138:319–344
22. Claeys M, van Steen E (2004) Basic studies. In: Steynberg AP, Dry ME (eds) Fischer-Tropsch technology, vol 152. Elsevie, pp 601–680
23. Schulz H (2003) Major and minor reactions in Fischer-Tropsch synthesis on cobalt catalysts. Top Catal 26:73–85
24. Dry ME (1982) Catalytic aspects of industrial Fischer-Tropsch synthesis. J Mol Catal 17:133–144
25. Schulz H (2013) Principles of Fischer-Tropsch synthesis—constraints on essential reactions ruling FT-selectivity. Catal Today 214:140–151
26. Weststrate CJ, van Helden P, van de Loosdrecht J, Niemantsverdriet JW (2015) Elemen-tary steps in Fischer-Tropsch synthesis: CO bond scission, CO oxidation and surface carbiding on Co(0001). Surf Sci 648:1–7

27. Iglesias González M, Kraushaar-Czarnetzki B, Schaub G (2011) Process comparison of biomass-to-liquid (BtL) routes Fischer-Tropsch synthesis and methanol to gasoline. Biomass Conver Biorefin 1:229–243
28. Project funding website. https://www.energiesystem-forschung.de/forschen/projekte/powerfuel. Last accessed 31 Jul 2023
29. Project website. https://www.elab2.kit.edu/index.php. Last accessed 31 Jul 2023
30. Kopernikus Press release. https://www.kopernikus-projekte.de/aktuelles/news/p2x_erste_strom_zu_kraftstoff_anlage_in_betrieb. Last accessed 31 Jul 2023
31. Pandiyan A, Kyriakou V, Neagu D, Welzel S, Goede A, van de Sanden MCM, Tsampas MN (2022) CO_2 conversion via coupled plasma-electrolysis process. J CO_2 Utilization 57:101904. https://doi.org/10.1016/j.jcou.2022.101904
32. Stadler TJ, Bender LJ, Pfeifer P (2022) Dynamic simulation of a compact sorption-enhanced water-gas shift reactor. Front Chem Eng 4. https://doi.org/10.3389/fceng.2022.1000064
33. Stadler TJ, Bertin-Mente B, Dittmeyer R, Brübach L, Böltken T, Pfeifer P (2022) Influence of CO_2-rich syngas on the selectivity to C_{10}–C_{14} in a coupled Fischer-Tropsch/hydrocracking process. Chem Ing Tec 94:289–298. https://doi.org/10.1002/cite.202100172
34. Welzel S, Pfeifer P (2023) Highlights from KEROGREEN's plasma route towards e-Kerosene. In: Final project event 27th September 2022 at KIT Germany. https://www.kerogreen.eu/downloads/220927_Final_event_Peter_Stefan_wo_video.pdf. Last accessed 31 Jul 2023
35. Wolf M, Fischer N, Claeys M (2021) Formation of metal-support compounds in cobalt-based Fischer-Tropsch synthesis: a review. Chem Catalysis 1(5):1014–1041. https://doi.org/10.1016/j.checat.2021.08.002
36. Pöchlauer P, Bohn L, Kotthaus M, Kraut M, Vorbach M, Wenka A, Schubert KF (2006) Micro-structured devices for the chemical research, process development, and production-opportunities and limits. In: Micro-structured devices for chemical research. Process development and production—opportunities and limits, F. Hoffmann-La Roche Ltd., Basel
37. Suo Y, Yao Y, Zhang Y, Xing S, Yuan Z-Y (2022) Recent advances in cobalt-based Fischer-Tropsch synthesis catalysts. J Ind Eng Chem 115:92–119. https://doi.org/10.1016/j.jiec.2022.08.026
38. van Ravenhorst IK, Vogt C, Oosterbeek H, Bossers KW, Moya-Cancino JG, van Bavel AP, van der Eerden AMJ, Vine D, de Groot FMF, Meirer F, Weckhuysen BM (2018) Capturing the genesis of an active Fischer-Tropsch synthesis catalyst with operando X-ray nanospectroscopy. Angew Chem Int Ed 57:11957. https://doi.org/10.1002/anie.201806354
39. Loewert M, Serrer M-A, Carambia T, Stehle M, Zimina CA, Kalz KF, Lichtenberg H, Saraçi E, Pfeifer P, Grunwaldt J-D (2020) Bridging the gap between industry and synchrotron: an operando study at 30 bar over 300 h during Fischer–Tropsch synthesis. React Chem Eng 5:1071–1082. https://doi.org/10.1039/C9RE00493A
40. Fischer N, Claeys M (2020) In situ characterization of Fischer-Tropsch catalysts: a review. J Phys D: Appl Phys 53:293001. https://doi.org/10.1088/1361-6463/ab761c
41. Wolf M, Fischer N, Claeys M (2020) Water-induced deactivation of cobalt-based Fischer-Tropsch catalysts. Nat Catal 3:962–965. https://doi.org/10.1038/s41929-020-00534-5
42. Claeys M, Dry ME, van Steen E, du Plessis E, van Berge PJ, Saib AM, Moodley DJ (2014) In situ magnetometer study on the formation and stability of cobalt carbide in Fischer-Tropsch synthesis. J Catal 318:193–202. https://doi.org/10.1016/j.jcat.2014.08.002
43. https://care-o-sene.com/en/. Last access 29 Jul 2023
44. Rytter E, Holmen A (2015) Deactivation and regeneration of commercial type Fischer-Tropsch co-catalysts—a mini-review. Catalysts 5:478–499. https://doi.org/10.3390/catal5020478
45. Claeys M, van Steen E, Botha T, Crous R, Ferreira A, Harilal A (2021) Oxidation of Hägg carbide during high-temperature Fischer–Tropsch synthesis: size-dependent thermodynamics and in situ observations. ACS Catal 11(22):13866–13879. https://pubs.acs.org/doi/abs/10.1021/acscatal.1c03719
46. Bier W, Keller W, Linder G, Seidel D, Schubert K (1990) Manufacturing and testing of compact micro heat exchangers with high volumetric heat transfer coefficients. Microstruct Sens Actuators, DSC 19:189–197

47. Ramshaw C (ed) (1995) 1st international conference on process intensification for the chemical industry, Antwerp, Belgium (6–8 Dec 1995). BHR group conference series. Publication No. 18. Mechanical Engineering Publications Limited, London
48. Ramshaw C (1983) Chem Eng 389(2):13–14
49. Lerou JJ, Tonkovich AL, Silva L, Perry S, McDaniel J (2010) Microchannel reactor architecture enables greener processes. Chem Eng Sci 65:380–385
50. Tonkovich A, Kuhlmann D, Rogers A, McDaniel J, Fitzgerald S, Arora R, Yuschak T (2005) Microchannel technology scale-up to commercial capacity. Chem Eng Res Des 83(6):634–639. https://doi.org/10.1205/cherd.04354
51. Kee RJ, Karakaya C, Zhu H (2017) Process intensification in the catalytic conversion of natural gas to fuels and chemicals. Proc Combust Inst 36(1):51–76. https://doi.org/10.1016/j.proci.2016.06.014
52. Myrstad R, Eri S, Pfeifer P, Rytter E, Holmen A (2009) Fischer-Tropsch synthesis in a microstructured reactor. Catal Today 147:S301–S304. https://doi.org/10.1016/j.cattod.2009.07.011
53. Piermartini P, Böltken T, Selinsek M, Pfeifer P (2017) Influence of channel geometry on Fischer-Tropsch synthesis in microstructured reactors. Chem Eng J 313:328–335. https://doi.org/10.1016/j.cej.2016.12.076
54. Knochen J, Güttel R, Knobloch C, Turek T (2010) Fischer-Tropsch synthesis in milli-structured fixed-bed reactors: experimental study and scale-up considerations. Chem Eng Process 49(9):958–964. https://doi.org/10.1016/j.cep.2010.04.013
55. Chambrey S, Fongarland P, Karaca H, Piché S, Griboval-Constant A, Schweich D, Luck F, Savin S, Khodakov AY (2011) Fischer-Tropsch synthesis in milli-fixed bed reactor: comparison with centimetric fixed bed and slurry stirred tank reactors. Catal Today 171(1):201–206. https://doi.org/10.1016/j.cattod.2011.04.046
56. Chin Y-H, Hu J, Cao C, Gao Y, Wang Y (2005) Preparation of a novel structured catalyst based on aligned carbon nanotube arrays for a microchannel Fischer-Tropsch synthesis reactor. Catal Today 110(1–2):47–52. https://doi.org/10.1016/j.cattod.2005.09.007
57. Almeida LC, Sanz O, Merino D, Arzamendi G, Gandía LM, Montes M (2013) Kinetic analysis and microstructured reactors modeling for the Fischer-Tropsch synthesis over a Co–Re/Al2O3 catalyst. Catal Today 215:103–111. https://doi.org/10.1016/j.cattod.2013.04.021
58. Almeida LC, Sanz O, D'olhaberriague J, Yunes S, Montes M (2013) Microchannel reactor for Fischer-Tropsch synthesis: adaptation of a commercial unit for testing microchannel blocks. Fuel 110:171–177. https://doi.org/10.1016/j.fuel.2012.09.063
59. Klemm E, Döring H, Geißelmann A, Schirrmeister S (2007) Mikrostrukturreaktoren für die heterogene Katalyse. Chemie Ingenieur Technik 79:697–706. https://doi.org/10.1002/cite.200700052
60. Vogel AP, van Dyk B, Saib AM (2016) GTL using efficient cobalt Fischer-Tropsch catalysts. Catal Today 259(Part 2):323–330. https://doi.org/10.1016/j.cattod.2015.06.018
61. Ying X, Zhang L, Xu H, Ren Y-L, Luo Q, Zhu H-W, Qu H, Xuan J (2016) Efficient Fischer-Tropsch microreactor with innovative aluminizing pretreatment on stainless steel substrate for Co/Al2O3 catalyst coating. Fuel Process Technol 143:51–59. https://doi.org/10.1016/j.fuproc.2015.11.005
62. Sun Y, Jia Z, Yang G, Zhang L, Sun Z (2017) Fischer-Tropsch synthesis using iron based catalyst in a microchannel reactor: performance evaluation and kinetic modeling. Int J Hydrogen Energy 42:49, 29222–29235. https://doi.org/10.1016/j.ijhydene.2017.10.022
63. Zhang X, Zhong L, Zeng G, Gu Y, Peng C, Yu F, Tang Z, Sun Y (2018) Process intensification of honeycomb fractal micro-reactor for the direct production of lower olefins from syngas. Chem Eng J 351:12–21. https://doi.org/10.1016/j.cej.2018.06.078
64. Cao C, Hu J, Li S, Wilcox W, Wang Y (2009) Intensified Fischer-Tropsch synthesis process with microchannel catalytic reactors. Catal Today 140(3–4):149–156. https://doi.org/10.1016/j.cattod.2008.10.016
65. Loewert M, Hoffmann J, Piermartini P, Selinsek M, Dittmeyer R, Pfeifer P (2019) Microstructured Fischer-Tropsch reactor scale-up and opportunities for decentralized application. Chem Eng Technol 42:2202–2214. https://doi.org/10.1002/ceat.201900136

66. Steynberg AP, Deshmukh SR, Robota HJ (2018) Fischer-Tropsch catalyst deactivation in commercial microchannel reactor operation. Catal Today 299:10–13. https://doi.org/10.1016/j.cattod.2017.05.064
67. https://www.edwardtdodge.com/2014/10/31/velocys-small-scale-gas-to-liquids/. Last accessed 30 Jul 2023
68. Jung I, Na J, Park S, Jeon J, Mo Y-G, Yi J-Y, Chung J-T, Han C (2017) Optimal design of a large scale Fischer-Tropsch microchannel reactor module using a cell-coupling method. Fuel Process Technol 159:448–459. https://doi.org/10.1016/j.fuproc.2016.12.004
69. Mohammad N, Chukwudoro C, Bepari S, Basha O, Aravamudhan S, Kuila D (2022) Scale-up of high-pressure F-T synthesis in 3D printed stainless steel microchannel microreactors: experiments and modeling. Catal Today 397–399:182–196. https://doi.org/10.1016/j.cattod.2021.09.038
70. Na J, Kshetrimayum KS, Jung I, Park S, Lee Y, Kwon O, Mo Y, Chung J, Yi J, Lee U, Han C (2018) Optimal design and operation of Fischer-Tropsch microchannel reactor for pilot-scale compact gas-to-liquid process. Chem Eng Proc Proc Intensification 128:63–76. https://doi.org/10.1016/j.cep.2018.04.013
71. Pfeifer P, Schmidt S, Betzner F, Kollmann M, Loewert M, Böltken T, Piermartini P (2022) Scale-up of microstructured Fischer-Tropsch reactors—status and perspectives. Curr Opin Chem Eng 36:100776. https://doi.org/10.1016/j.coche.2021.100776
72. Mesheryakov D, Kirillov VA, Kuzin NA (1999) A multifunctional reactor with a regular catalyst packing for Fischer-Tropsch synthesis. Chem Eng Sci 54(10):1565–1570. https://doi.org/10.1016/S0009-2509(99)00066-4
73. de Deugd RM, Chougule RB, Kreutzer MT, Michiel Meeuse F, Grievink J, Kapteijn F, Moulijn JA (2003) Is a monolithic loop reactor a viable option for Fischer–Tropsch synthesis? Chem Eng Sci 58:3–6, 583–591. https://doi.org/10.1016/S0009-2509(02)00583-3
74. Maretto C, Krishna R (1999) Modelling of a bubble column slurry reactor for Fischer-Tropsch synthesis. Catal Today 52:279–289. https://doi.org/10.1016/S0920-5861(99)00082-6
75. Güttel R (2009) Monolith loop reactors for Fischer-Tropsch synthesis. Doctoral thesis, TU Clausthal
76. Vervloet D, Kapteijn F, Nijenhuis J, van Ommen JR (2012) Fischer-Tropsch reaction–diffusion in a cobalt catalyst particle: aspects of activity and selectivity for a variable chain growth probability. Catal Sci Technol 2:1221–1233. https://doi.org/10.1039/C2CY20060K
77. Merino D, Sanz O, Montes M (2017) Effect of catalyst layer macroporosity in high-thermal-conductivity monolithic Fischer-Tropsch catalysts. Fuel 210:49–57. https://doi.org/10.1016/j.fuel.2017.08.040
78. Visconti CG, Tronconi E, Groppi G, Lietti L, Iovane M, Rossini S, Zennaro R (2011) Monolithic catalysts with high thermal conductivity for the Fischer-Tropsch synthesis in tubular reactors. Chem Eng J 171(3):1294–1307. https://doi.org/10.1016/j.cej.2011.05.014
79. Fratalocchi L, Groppi G, Visconti CG, Lietti L, Tronconi E (2020) Adoption of 3D printed highly conductive periodic open cellular structures as an effective solution to enhance the heat transfer performances of compact Fischer-Tropsch fixed-bed reactors. Chem Eng J 386:123988. https://doi.org/10.1016/j.cej.2019.123988
80. Peacock M, Paterson J, Reed L, Davies S, Carter S, Coe A, Clarkson J (2020) Innovation in Fischer–Tropsch: developing fundamental understanding to support commercial opportunities. Top Catal 63:328–339. https://doi.org/10.1007/s11244-020-01239-6
81. Asalieva E, Gryaznov K, Kulchakovskaya E, Ermolaev I, Sineva L, Mordkovich V (2015) Fischer-Tropsch synthesis on cobalt-based catalysts with different thermally conductive additives. Appl Catal A 505:260–266. https://doi.org/10.1016/j.apcata.2015.08.006
82. Pangarkar K, Schildhauer TJ, van Ommen JR, Nijenhuis J, Moulijn JA, Kapteijn F (2009) Experimental and numerical comparison of structured packings with a randomly packed bed reactor for Fischer-Tropsch synthesis. Catal Today 147S:S2–S9. https://doi.org/10.1016/j.cattod.2009.07.035
83. Fratalocchi L, Visconti CG, Groppi G, Lietti L, Tronconi E (2018) Intensifying heat transfer in Fischer-Tropsch tubular reactors through the adoption of conductive packed foams. Chem Eng J 349:829–837. https://doi.org/10.1016/j.cej.2018.05.108

84. Fratalocchi L, Visconti CG, Groppi G, Lietti L, Tronconi E (2022) Packed-POCS with skin: a novel concept for the intensification of non-adiabatic catalytic processes demonstrated in the case of the Fischer-Tropsch synthesis. Catal Today 383:15–20. https://doi.org/10.1016/j.cattod.2020.12.031
85. Hooshyar N, Vervloet D, Kapteijn F, Hamersma PJ, Mudde RF, van Ommen JR (2012) Intensifying the Fischer-Tropsch synthesis by reactor structuring—a model study. Chem Eng J 207–208:865–870. https://doi.org/10.1016/j.cej.2012.07.105
86. Frost L, Hartvigsen J, Elangovan D (2011) Development of a compact Fischer Tropsch reactor. In: Conference paper from 2011 AIChE annual meeting, assessed 31.07.2022 via https://www.researchgate.net/profile/Lyman-Frost/publication/267313463_Development_of_a_Compact_Fischer_Tropsch_Reactor/links/55491e1b0cf2ebfd8e3ad82e/Development-of-a-Compact-Fischer-Tropsch-Reactor.pdf
87. Barrera JL, Hartvigsen JJ, Hollist M, Pike J, Yarosh A, Fullilove NP, Beck VA (2023) Design optimization of integrated cooling inserts in modular Fischer-Tropsch reactors. Chem Eng Sci 268:118423. https://doi.org/10.1016/j.ces.2022.118423
88. Kapteijn F, Moulijn JA (2022) Structured catalysts and reactors—perspectives for demanding applications. Catal Today 383:5–14. https://doi.org/10.1016/j.cattod.2020.09.026
89. Odunsi AO, O'Donovan TS, Reay DA (2016) Temperature stabilisation in Fischer-Tropsch reactors using phase change material (PCM). Appl Therm Eng 93:1377–1393. https://doi.org/10.1016/j.applthermaleng.2015.08.084
90. An M, Guan X, Yang N, Bu Y, Xu M, Men Z (2018) Effects of internals on fluid dynamics and reactions in pilot-scale slurry bubble column reactors: a CFD study for Fischer-Tropsch synthesis. Chem Eng Proc Proc Intensification 132:194–207. https://doi.org/10.1016/j.cep.2018.09.004
91. Geng S, Mao Z-S, Huang Q, Yang C (2021) Process intensification in pneumatically agitated slurry reactors. Engineering 7(3):304–325. https://doi.org/10.1016/j.eng.2021.03.002
92. Abbaslou RMM, Mohammadzadeh JSS, Dalai AK (2009) Review on Fischer-Tropsch synthesis in supercritical media. Fuel Proc Technol 90(7–8):849–856. https://doi.org/10.1016/j.fuproc.2009.03.018
93. Mogalicherla AK, Elmalik EE, Elbashir NO (2012) Enhancement in the intraparticle diffusion in the supercritical phase Fischer-Tropsch synthesis. Chem Eng Process 62:59–68. https://doi.org/10.1016/j.cep.2012.09.008
94. Abusrafa AE, Challiwala MS, Choudhury HA, Wilhite BA, Elbashir NO (2020) Experimental verification of 2-dimensional computational fluid dynamics modeling of supercritical fluids Fischer Tropsch reactor bed. Catal Today 343:165–175. https://doi.org/10.1016/j.cattod.2019.05.027
95. Sun C, Luo Z, Choudhary A, Pfeifer P, Dittmeyer R (2017) Influence of the condensable hydrocarbons on an integrated Fischer-Tropsch synthesis and hydrocracking process: simulation and experimental validation. Ind Eng Chem Res 56:13075–13085. https://doi.org/10.1021/acs.iecr.7b01326
96. Sun C, Pfeifer P, Dittmeyer R (2017) One-stage syngas-to-fuel in a micro-structured reactor: investigation of integration pattern and operating conditions on the selectivity and productivity of liquid fuels. Chem Eng J 326:37–46. https://doi.org/10.1016/j.cej.2017.05.133
97. Sun C, Zhan T, Pfeifer P, Dittmeyer R (2017) Influence of Fischer-Tropsch synthesis (FTS) and hydrocracking (HC) conditions on the product distribution of an integrated FTS-HC process. Chem Eng J 310:272–281. https://doi.org/10.1016/j.cej.2016.10.118
98. Sun C, Klumpp M, Binder JR, Pfeifer P, Dittmeyer R (2017) Einstufige Treibstoffsynthese mittels gedruckter Katalysatorschichten in mikrostrukturierten Reaktoren = one-stage syngas-to-fuel conversion with printed catalyst layers in microstructured reactors. Chemie - Ingenieur - Technik 89(7):894–902. https://doi.org/10.1002/cite.201600180
99. Zhu C, Gamliel DP, Valla JA, Bollas GM (2021) Fischer-Tropsch synthesis in monolith catalysts coated with hierarchical ZSM-5. Appl Catal B 284:119719. https://doi.org/10.1016/j.apcatb.2020.119719

100. Zhu C, Bollas GM (2018) Gasoline selective Fischer-Tropsch synthesis in structured bifunctional catalysts. Appl Catal B 235:92–102. https://doi.org/10.1016/j.apcatb.2018.04.063
101. Kirsch H, Sommer U, Pfeifer P, Dittmeyer R (2020) Power-to-fuel conversion based on reverse water-gas-shift, Fischer-Tropsch synthesis and hydrocracking: mathematical modeling and simulation in Matlab/Simulink. Chem Eng Sci 227:115930. https://doi.org/10.1016/j.ces.2020.115930
102. Kirsch H, Lochmahr N, Staudt C, Pfeifer P (2020) Dittmeyer, production of CO_2-neutral liquid fuels by integrating Fischer-Tropsch synthesis and hydrocracking in a single micro-structured reactor: Performance evaluation of different configurations by factorial design experiments. Chem. Eng J 393:124553. https://doi.org/10.1016/j.cej.2020.124553
103. Brosius R (2019) WO/2020/016845, Low pressure hydrocracking process for the production of a high yield of middle distillates from a high boiling hydrocarbon feedstock, 19 Jul 2019
104. Rytter E (2006) WO2008/062208, Multi stage process for producing hydrocarbons from syngas, 23 Nov 2006
105. Pandey U, Putta KR, Rout KR, Blekkan EA, Rytter E, Hillestad M (2022) Staging and path optimization of Fischer-Tropsch synthesis. Chem Eng Res Des 187:276–289. https://doi.org/10.1016/j.cherd.2022.08.033
106. Rafiee A, Hillestad M (2013) Staging of the Fischer-Tropsch reactor with a cobalt-based catalyst. Chem Eng Technol 36:1729–1738. https://doi.org/10.1002/ceat.201200700
107. Fischer F, Bahr T, Meusel A (1935) Über die katalytische Reduktion des Kohlendioxyds zu Methan und höheren Kohlenwasserstoffen bei gewöhnlichem Druck 16:466–469
108. Küster H (1936) Über die Reduktion der Kohlensäure zu höheren Kohlenwasserstoffen bei Atmosphärendruck an Katalysatoren der Eisengruppe. Brennst.-Chem. 17:221–228
109. Kölbel H, Ackermann P (1954) U.S. Patent 2,692,274
110. Russell WW, Miller GH (1950) Catalytic hydrogenation of carbon dioxide to higher hydrocarbons. J Am Chem Soc 72:2446–2454. https://doi.org/10.1021/ja01162a025
111. Weatherbee GD, Bartholomew CH (1984) Hydrogenation of CO_2 on group VIII metals: IV. Specific activities and selectivities of silica-supported Co, Fe, and Ru. J Catal 87:352–362. https://doi.org/10.1016/0021-9517(84)90196-9
112. Fiato RA, Soled SL, Rice GW, Miseo S (1992) U.S. Patent 5,140,049A
113. Lee M-D, Lee J-F, Chang C-S (1989) Hydrogenation of carbon dioxide on unpromoted and potassium-promoted iron catalysts. Bull Chem Soc Jpn 62:2756–2758. https://doi.org/10.1246/bcsj.62.2756
114. Lee J-F, Chern W-S, Lee M-D, Dong T-Y (1992) Hydrogenation of carbon dioxide on iron catalysts doubly promoted with manganese and potassium. Can J Chem Eng 70:511–515. https://doi.org/10.1002/cjce.5450700314
115. Dorner RW, Hardy DR, Williams FW, Willauer HD (2010) Heterogeneous catalytic CO_2 conversion to value-added hydrocarbons. Energy Environ Sci 3:884. https://doi.org/10.1039/c001514h
116. Wei J, Yao R, Han Y, Ge Q, Sun J (2021) Towards the development of the emerging process of CO_2 heterogenous hydrogenation into high-value unsaturated heavy hydrocarbons. Chem Soc Rev 50:10764–10805. https://doi.org/10.1039/D1CS00260K
117. Sai Prasad PS, Bae JW, Jun K-W, Lee K-W (2008) Fischer–Tropsch synthesis by carbon dioxide hydrogenation on Fe-based catalysts. Catal Surv Asia 12:170–183
118. Panzone C, Philippe R, Chappaz A, Fongarland P, Bengaouer A (2020) Power-to-liquid catalytic CO_2 valorization into fuels and chemicals: focus on the Fischer-Tropsch route. J CO_2 Util 38:314–347. https://doi.org/10.1016/j.jcou.2020.02.009
119. Wang D, Xie Z, Porosoff MD, Chen JG (2021) Recent advances in carbon dioxide hydrogenation to produce olefins and aromatics. Chem 7:2277–2311. https://doi.org/10.1016/j.chempr.2021.02.024
120. Ye R-P, Ding J, Gong W, Argyle MD, Zhong Q, Wang Y, Russell CK, Xu Z, Russell AG, Li Q, Fan M, Yao Y-G (2019) CO_2 hydrogenation to high-value products via heterogeneous catalysis. Nat Commun 10:5698. https://doi.org/10.1038/s41467-019-13638-9

121. Atsbha TA, Yoon T, Seongho P, Lee C-J (2021) A review on the catalytic conversion of CO_2 using H2 for synthesis of CO, methanol, and hydrocarbons. J CO_2 Util 44:101413. https://doi.org/10.1016/j.jcou.2020.101413
122. Riedel T, Schaub G, Jun K-W, Lee K-W (2001) Kinetics of CO_2 hydrogenation on a K-promoted Fe catalyst. Ind Eng Chem Res 40:1355–1363. https://doi.org/10.1021/ie000084k
123. Wei J, Ge Q, Yao R, Wen Z, Fang C, Guo L, Xu H, Sun J (2017) Directly converting CO_2 into a gasoline fuel. Nat Commun 8:15174. https://doi.org/10.1038/ncomms15174
124. Visconti CG, Martinelli M, Falbo L, Fratalocchi L, Lietti L (2016) CO_2 hydrogenation to hydrocarbons over Co and Fe-based Fischer-Tropsch catalysts. Catal Today 277:161–170. https://doi.org/10.1016/j.cattod.2016.04.010
125. Visconti CG, Martinelli M, Falbo L, Infantes-Molina A, Lietti L, Forzatti P, Iaquaniello G, Palo E, Picutti B, Brignoli F (2017) CO_2 hydrogenation to lower olefins on a high surface area K-promoted bulk Fe-catalyst. Appl Catal B 200:530–542. https://doi.org/10.1016/j.apcatb.2016.07.047
126. Riedel T, Schulz H, Schaub G, Jun K-W, Hwang J-S, Lee K-W (2003) Fischer-Tropsch on iron with H2/CO and H2/CO_2 as synthesis gases: the episodes of formation of the Fischer-Tropsch regime and construction of the catalyst. Top Catal 26:41–54. https://doi.org/10.1023/B:TOCA.0000012986.46680.28
127. Meiri N, Radus R, Herskowitz M (2017) Simulation of novel process of CO_2 conversion to liquid fuels. J CO_2 Util 17:284–289. https://doi.org/10.1016/j.jcou.2016.12.008
128. Landau MV, Vidruk R, Herskowitz M (2014) Sustainable production of green feed from carbon dioxide and hydrogen. Chemsuschem 7:785–794. https://doi.org/10.1002/cssc.201301181
129. Brübach L, Hodonj D, Pfeifer P (2022) Kinetic analysis of CO_2 hydrogenation to long-chain hydrocarbons on a supported iron catalyst. Ind Eng Chem Res 61:1644–1654. https://doi.org/10.1021/acs.iecr.1c04018
130. Brübach L, Hodonj D, Pfeifer P (2022) Kinetic analysis of CO_2 hydrogenation to long-chain hydrocarbons on a supported iron catalyst. Ind Eng Chem Res 61(4):1644–1654. https://pubs.acs.org/doi/10.1021/acs.iecr.1c04018
131. Iglesias MG, de Vries C, Claeys M, Schaub G (2015) Chemical energy storage in gaseous hydrocarbons via iron Fischer–Tropsch synthesis from H2/CO_2—kinetics, selectivity and process considerations. Catal Today 242:184–192. https://doi.org/10.1016/j.cattod.2014.05.020
132. Riedel T, Claeys M, Schulz H, Schaub G, Nam S-S, Jun K-W, Choi M-J, Kishan G, Lee K-W (1999) Comparative study of Fischer–Tropsch synthesis with H2/CO and H2/CO_2 syngas using Fe- and Co-based catalysts. Appl Catal A 186:201–213. https://doi.org/10.1016/S0926-860X(99)00173-8
133. Fischer N, Henkel R, Hettel B, Iglesias M, Schaub G, Claeys M (2016) Hydrocarbons via CO_2 hydrogenation over iron catalysts: the effect of potassium on structure and performance. Catal Lett 146:509–517. https://doi.org/10.1007/s10562-015-1670-9
134. Hong J-S, Hwang JS, Jun K-W, Sur JC, Lee K-W (2001) Deactivation study on a coprecipitated Fe-Cu-K-Al catalyst in CO_2 hydrogenation. Appl Catal A 218:53–59. https://doi.org/10.1016/S0926-860X(01)00617-2
135. Dry ME (2004) Chapter 7—FT catalysts. In: Steynberg A, Dry M (eds) Fischer-Tropsch technology, Reprinted, Elsevier, Amsterdam, pp 533–600
136. Bukur DB, Sivaraj C (2002) Supported iron catalysts for slurry phase Fischer–Tropsch synthesis. Appl Catal A 231:201–214. https://doi.org/10.1016/S0926-860X(02)00053-4
137. Choi PH, Jun K-W, Lee S-J, Choi M-J, Lee K-W (1996) Hydrogenation of carbon dioxide over alumina supported Fe-K catalysts. Catal Lett 40:115–118. https://doi.org/10.1007/BF00807467
138. Kuei C-K, Lee M-D (1991) Hydrogenation of carbon dioxide by hybrid catalysts, direct synthesis of aromatics from carbon dioxide and hydrogen. Can J Chem Eng 69:347–354. https://doi.org/10.1002/cjce.5450690142
139. Amoyal M, Vidruk-Nehemya R, Landau MV, Herskowitz M (2017) Effect of potassium on the active phases of Fe catalysts for carbon dioxide conversion to liquid fuels through hydrogenation. J Catal 348:29–39. https://doi.org/10.1016/j.jcat.2017.01.020

140. Martinelli M, Visconti CG, Lietti L, Forzatti P, Bassano C, Deiana P (2014) CO_2 reactivity on Fe–Zn–Cu–K Fischer-Tropsch synthesis catalysts with different K-loadings. Catal Today 228:77–88. https://doi.org/10.1016/j.cattod.2013.11.018
141. Rodemerck U, Holeňa M, Wagner E, Smejkal Q, Barkschat A, Baerns M (2013) Catalyst development for CO_2 hydrogenation to fuels. ChemCatChem 5:1948–1955. https://doi.org/10.1002/cctc.201200879
142. Satthawong R, Koizumi N, Song C, Prasassarakich P (2013) Bimetallic Fe–Co catalysts for CO_2 hydrogenation to higher hydrocarbons. J CO_2 Util 3–4:102–106. https://doi.org/10.1016/j.jcou.2013.10.002
143. Liang B, Duan H, Sun T, Ma J, Liu X, Xu J, Su X, Huang Y, Zhang T (2019) Effect of Na promoter on Fe-based catalyst for CO 2 hydrogenation to alkenes. ACS Sustain Chem Eng 7:925–932. https://doi.org/10.1021/acssuschemeng.8b04538
144. Wei J, Sun J, Wen Z, Fang C, Ge Q, Xu H (2016) New insights into the effect of sodium on Fe 3 O 4—based nanocatalysts for CO 2 hydrogenation to light olefins. Catal Sci Technol 6:4786–4793. https://doi.org/10.1039/C6CY00160B
145. Liu X, Zhang C, Tian P, Xu M, Cao C, Yang Z, Zhu M, Xu J (2021) Revealing the effect of sodium on iron-based catalysts for CO_2 hydrogenation: insights from calculation and experiment. J Phys Chem C 125:7637–7646. https://doi.org/10.1021/acs.jpcc.0c11123
146. Liu B, Geng S, Zheng J, Jia X, Jiang F, Liu X (2018) Unravelling the new roles of Na and Mn promoter in CO 2 hydrogenation over Fe 3 O 4 -based catalysts for enhanced selectivity to light α-olefins. ChemCatChem 10:4718–4732. https://doi.org/10.1002/cctc.201800782
147. Schmidt C, Kureti S (2022) CO 2 conversion by Fischer-Tropsch synthesis using na-modified Fe catalysts. Chem Ing Tech cite 202200067. https://doi.org/10.1002/cite.202200067
148. Wen C, Jiang J, Chiliu C, Tian Z, Xu X, Wu J, Wang C, Ma L (2020) Single-step selective conversion of carbon dioxide to aromatics over Na-Fe 3 O 4 /hierarchical HZSM-5 zeolite catalyst. Energy Fuels 34:11282–11289. https://doi.org/10.1021/acs.energyfuels.0c02120
149. Wang Y, Kazumi S, Gao W, Gao X, Li H, Guo X, Yoneyama Y, Yang G, Tsubaki N (2020) Direct conversion of CO_2 to aromatics with high yield via a modified Fischer-Tropsch synthesis pathway. Appl Catal B 269:118792. https://doi.org/10.1016/j.apcatb.2020.118792
150. Khangale PR, Meijboom R, Jalama K (2020) CO_2 hydrogenation to liquid hydrocarbons via modified Fischer–Tropsch over alumina-supported cobalt catalysts: effect of operating temperature, pressure and potassium loading. J CO_2 Util 41:101268. https://doi.org/10.1016/j.jcou.2020.101268
151. Jo H, Khan MK, Irshad M, Arshad MW, Kim SK, Kim J (2022) Unraveling the role of cobalt in the direct conversion of CO_2 to high-yield liquid fuels and lube base oil. Appl Catal B 305:121041. https://doi.org/10.1016/j.apcatb.2021.121041
152. Shi Z, Yang H, Gao P, Li X, Zhong L, Wang H, Liu H, Wei W, Sun Y (2018) Direct conversion of CO_2 to long-chain hydrocarbon fuels over K–promoted CoCu/TiO_2 catalysts. Catal Today 311:65–73. https://doi.org/10.1016/j.cattod.2017.09.053
153. Choi MJ, Kim J, Lee S, Lee W, Lee K (2003) Promotion of CO_2 hydrogenation in fixed bed recycle reactors. In: Gale J, Kaya Y (eds) Greenhouse gas control technologies: proceedings of the 6th international conference on greenhouse gas control technologies, 1–4 October 2002, Kyoto, Japan, Pergamon, Amsterdam, Oxford, pp 1491–1496
154. Willauer HD, Bradley MJ, Baldwin JW, Hartvigsen JJ, Frost L, Morse JR, DiMascio F, Hardy DR, Hasler DJ (2020) Evaluation of CO_2 hydrogenation in a modular fixed-bed reactor prototype. Catalysts 10:970. https://doi.org/10.3390/catal10090970
155. Rohde MP, Unruh D, Schaub G (2005) Membrane application in fischer−tropsch synthesis to enhance CO 2 Hydrogenation. Ind Eng Chem Res 44:9653–9658
156. Li Z, Deng Y, Dewangan N, Hu J, Wang Z, Tan X, Liu S, Kawi S (2021) High temperature water permeable membrane reactors for CO_2 utilization. Chem Eng J 420:129834. https://doi.org/10.1016/j.cej.2021.129834
157. Steynberg AP, Dry ME, Davis BH, Breman BB (2004) Chapter 2—Fischer-Tropsch reactors. In: Steynberg A, Dry M (eds),Fischer-Tropsch technology, Reprinted, Elsevier, Amsterdam, pp 64–195

158. Kim J-S, Lee S, Lee S-B, Choi M-J, Lee K-W (2006) Performance of catalytic reactors for the hydrogenation of CO_2 to hydrocarbons. Catal Today 115:228–234. https://doi.org/10.1016/j.cattod.2006.02.038
159. Brübach L, Hodonj D, Biffar L, Pfeifer P (2022) Detailed Kinetic modeling of CO_2-based Fischer-Tropsch synthesis. Catalysts 12:630. https://doi.org/10.3390/catal12060630
160. de Klerk A (2011) Fischer-Tropsch refining, 1st edn. Wiley-VCH, Weinheim
161. Willauer HD, Ananth R, Olsen MT, Drab DM, Hardy DR, Williams FW (2013) Modeling and kinetic analysis of CO_2 hydrogenation using a Mn and K-promoted Fe catalyst in a fixed-bed reactor. J CO_2 Util 3–4:56–64. https://doi.org/10.1016/j.jcou.2013.10.003
162. Landau MV, Meiri N, Utsis N, Vidruk Nehemya R, Herskowitz M (2017) Conversion of CO_2, CO, and H_2 in CO_2 hydrogenation to fungible liquid fuels on Fe-based catalysts. Ind Eng Chem Res 56:13334–13355. https://doi.org/10.1021/acs.iecr.7b01817
163. de Klerk A (2011) Fischer-Tropsch fuels refinery design. Energy Environ Sci 4:1177–1205
164. de Klerk A (2008) Hydroprocessing peculiarities of Fischer-Tropsch syncrude. Catal Today 130:439–445. https://doi.org/10.1016/j.cattod.2007.10.006
165. Nel RJJ, de Klerk A (2007) Fischer−Tropsch aqueous phase refining by catalytic alcohol dehydration. Ind Eng Chem Res 46:3558–3565. https://doi.org/10.1021/ie061555r
166. Pfeifer P, Biffar L, Timm F, Böltken T (2020) Influence of power-to-fuel plant flexibility towards power and plant utilization and intermediate hydrogen buffer size. Chem Ing Tec 92:1976–1982. https://doi.org/10.1002/cite.202000084
167. González MJ, Schaub G (2015) Fischer-Tropsch synthesis with H_2/CO_2—catalyst behavior under transient conditions. Chem Ing Tec 87:848–854. https://doi.org/10.1002/cite.201400137
168. Bremaud M, Fongarland P, Anfray J, Jallais S, Schweich D, Khodakov AY (2005) Influence of syngas composition on the transient behavior of a Fischer-Tropsch continuous slurry reactor. Catal Today 106(1–4):137–142. https://doi.org/10.1016/j.cattod.2005.07.126
169. Loewert M, Pfeifer P (2020) Dynamically operated fischer-tropsch synthesis in PtL-Part 1: system response on intermittent feed. Chem Eng 4:2, 21. https://doi.org/10.3390/chemengineering4020021
170. Eilers H, González MJ, Schaub G (2016) Lab-scale experimental studies of Fischer-Tropsch kinetics in a three-phase slurry reactor under transient reaction conditions. Catal Today 275:164–171. https://doi.org/10.1016/j.cattod.2015.11.011
171. Loewert M, Riedinger M, Pfeifer P (2020) Dynamically operated Fischer–Tropsch synthesis in PtL—Part 2: coping with real PV profiles. Chem Eng 4:2, 27. https://doi.org/10.3390/chemengineering4020027
172. Nikačević N, Todić B, Mandić M, Petkovska M, Bukur DB (2020) Optimization of forced periodic operations in milli-scale fixed bed reactor for Fischer-Tropsch synthesis. Catal Today 343:156–164. https://doi.org/10.1016/j.cattod.2018.12.032
173. Mandić M, Dikić V, Petkovska M, Todić B, Bukur DB, Nikačević NM (2018) Dynamic analysis of millimetre-scale fixed bed reactors for Fischer-Tropsch synthesis. Chem Eng Sci 192:434–447. https://doi.org/10.1016/j.ces.2018.07.052
174. Wentrup J, Pesch GR, Thöming J (2022) Dynamic operation of Fischer-Tropsch reactors for power-to-liquid concepts: a review. Renew Sustain Energy Rev 162:112454. https://doi.org/10.1016/j.rser.2022.112454
175. de Swart JWA, Krishna R (2002) Simulation of the transient and steady state behaviour of a bubble column slurry reactor for Fischer-Tropsch synthesis. Chem Eng Process 41(1):35–47. https://doi.org/10.1016/S0255-2701(00)00159-8
176. Saeidi S, Nikoo MK, Mirvakili A, Bahrani S, Amin NAS, Rahimpour MR (2015) Recent advances in reactors for low-temperature Fischer-Tropsch synthesis: process intensification perspective. Rev Chem Eng 31(3):209–238. https://doi.org/10.1515/revce-2014-0042
177. Venvik HJ, Yang J (2017) Catalysis in microstructured reactors: short review on small-scale syngas production and further conversion into methanol, DME and Fischer-Tropsch products. Catal Today 285:135–146. https://doi.org/10.1016/j.cattod.2017.02.014

178. Holmen A, Venvik HJ, Myrstad R, Zhu J, Chen D (2013) Monolithic, microchannel and carbon nanofibers/carbon felt reactors for syngas conversion by Fischer-Tropsch synthesis. Catal Today 216:150–157. https://doi.org/10.1016/j.cattod.2013.06.006
179. Press release InfraServ, 20.04.2023. https://www.infraserv.com/en/news/presse/press-releases/pressemeldung-nc_62848.html. Last accessed 04 Aug 2023
180. Sheehan SW, Chen C, US20230234037, Molybdenum-based catalysts for carbon dioxide conversion, 05 May 2021
181. Sheehan SW, Chen C, Garedew-Ballard M, Luthria N, Shah MR, Wu Q (2023) WO2023137002, Methods and catalysts for carbon dioxide conversion to long-chain hydrocarbons, 10 Jan 2023
182. Press release Sasol, 06.09.2021. https://www.sasol.com/media-centre/media-releases/sasol-and-uct-researchers-collaborate-use-commercial-iron-catalysts. Last accessed 04 Aug 2023
183. Jürgens S, Oßwald P, Selinsek M, Piermartini P, Schwab J, Pfeifer P, Bauder U, Ruoff S, Rauch B, Köhler M (2019) Assessment of combustion properties of non-hydroprocessed Fischer-Tropsch Fuels for aviation. Fuel Process Technol 193:232–243. https://doi.org/10.1016/j.fuproc.2019.05.015
184. Voigt C, Kleine J, Sauer D, Moore RH, Bräuer T, Le Clercq P, Kaufmann MS, Jurkat-Witschas T, Aigner M, Bauder U, Boose Y, Borrmann S, Crosbie E, Diskin GS, DiGangi J, Hahn V, Heckl C, Huber F, Nowak JB, Rapp M, Rauch B, Robinson C, Schripp T, Shook M, Winstead E, Ziemba L, Schlager H, Anderson BE (2021) Cleaner burning aviation fuels can reduce contrail cloudiness. Commun Earth Environ 2:114. https://doi.org/10.1038/s43247-021-00174-y